SOME ASPECTS OF TIME DOMAIN REFLECTOMETRY (TDR), NEUTRON SCATTERING, and CAPACITANCE METHODS of SOIL WATER CONTENT MEASUREMENT*

S.R. EVETT
USDA-ARS
Bushland, Texas, USA

Pp. 5-49 *In* Comparison of soil water measurement using the neutron scattering, time domain reflectometry and capacitance methods. International Atomic Energy Agency, Vienna, Austria, IAEA-TECDOC-1137. 2000.

Abstract

Soil water measurement methods encounter particular problems related to the physics of each method. For TDR, these relate to wave form shape changes caused by soil, soil water, and TDR probe properties. Methods of wave form interpretation that overcome these problems are discussed and specific computer algorithms are presented. Neutron scattering is well understood, but calibration methods remain critical to accuracy and precision, and are discussed with recommendations for field calibration and use. Capacitance probes tend to exhibit very small radii of influence and thus are sensitive to small scale changes in soil properties, and are difficult or impossible to field calibrate. Field comparisons of neutron and capacitance probes are presented.

Table of Contents

Mailing address is P.O. Drawer 10, Bushland, Texas, 79012, USA. E-mail address is srevett@ag.gov and Internet location is http://www.cprl.ars.usda.gov/programs.

1. AUTOMATIC TDR WAVE FORM INTERPRETATION

Time domain reflectometry became known as a useful method for soil water content and bulk electrical conductivity measurement in the 1980s through the publication of a series of papers by Topp, Dalton, Dasberg and others [1,2,3,4,5]. Automated TDR systems for water content measurement were described in the late 1980s and early 1990s by Baker and Allmaras [6], Heimovaara and Bouten [7], Herkelrath et al. [8], Evett et al. [9], and Evett [10]. Commercial systems became available in the late 1980s and continue to evolve with TDR probes, multiplexers, and instruments available from a few companies, usually with proprietary and fairly rudimentary software interfaces embedded in proprietary data acquisition units. A few papers have been published describing some aspects of wave form interpretation, notably Topp et al. [11], Baker and Allmaras [6], and Heimovaara [12]. Evett [13] described the TACQ computer program for controlling an automatic TDR system and interpreting wave forms. Wave form interpretation is a particular difficulty of the TDR method, and robust computer algorithms for interpretation are critical for unattended, automatic data acquisition. Several soil, soil water, and TDR probe properties influence wave form shape and the robustness of interpretation methods, and are discussed here. Discussion continues on graphical algorithms for automated wave form interpretation, used in the TACQ program, that respond to these influences.

1.1. **The TDR wave form and relationship to the probe**

In the TDR method, a very fast rise time (approx. 200 ps) step voltage increase is injected into a wave guide (usually coaxial cable) that carries this pulse to a probe placed in the soil or other porous medium. In a typical field installation, the probe is connected to the instrument through a network of coaxial cables and multiplexers. Part of the TDR instrument (e.g., Tektronix TDR cable tester) provides the voltage step and another part, essentially a fast oscilloscope, captures the reflected wave form. The oscilloscope can capture wave forms that represent all, or any part of, the wave guide (this includes cables, multiplexers and probes), beginning from a location that is actually inside the instrument and ending at the instrument's range (e.g., 500 m or about 5.5 microseconds for a Tektronix cable tester).

For example, Fig. 1 shows a wave form that represents the wave guide from a point inside the cable tester, before the step pulse is injected, and extending beyond the pulse injection point to a point along the cable that is 4.5 m from the cable tester. The step nature of the pulse is clear. The relative height of the wave form represents a voltage, which is proportional to the impedance of the wave guide. Although most TDR instruments display the horizontal axis in units of length (a holdover from the primary use of these instruments in detecting the location of cable faults), the horizontal axis is actually measured in units of time. The TDR instrument converts the time measurement to length units by using the relative propagation velocity factor, Vp (dimensionless), which is a fraction of the speed of light in a vacuum. For a given cable, the correct value of Vp is inversely proportional to the permittivity, ε (dimensionless), of the dielectric (insulating plastic) between the inner and outer conductors of the cable

$$Vp = v/c_o = (\varepsilon\mu)^{-0.5} \quad (1)$$

where v is the propagation velocity (m s^{-1}) of the pulse along the cable, c_o is the speed (m s^{-1}) of light in a vacuum, and μ (dimensionless) is the magnetic permeability (usually very close to unity) of the dielectric material. The amount of the wave form visible on the screen is determined by both the Vp and the distance per division settings, the latter of which determines the width of the instrument display in length units.

The TDR method relies on graphical interpretation of the wave form reflected from just that part of the wave guide that is the probe (Fig. 2). Baker and Allmaras [6] described how the first derivative of the wave form could be used to find some of the important features related to travel time of the step pulse. These and other features are illustrated in Figure 3. An example of graphical interpretation of the wave form for a 20-cm TDR probe in wet sand shows how tangent lines may be

fitted to several wave form features (Fig. 4). Intersections of the tangent lines define times related to i) the separation of the outer braid from the coaxial cable so that it can be connected to one of the probe rods, t1.bis; ii) the time when the pulse exits the handle and enters the soil, t1; and iii) the time when the pulse reaches the ends of the probe rods, t2 (all in s). The time taken for the step voltage pulse to travel along the probe rods, t_t = t2 - t1, is related to the propagation velocity as

$$t_t = 2L/v \quad (2)$$

where L is the length (m) of the rods (Fig. 2), and the factor 2 is due to the time being for two-way travel.

For a TDR probe in a soil, the dielectric is a complex mixture of air, water and soil particles that exhibits an apparent permittivity, ε_a. Substituting ε_a and Eq. 2 into Eq. 1, and assuming $\mu = 1$, we see that ε_a may be determined for a probe of known length, L, by measuring t_t

$$\varepsilon_a = [c_o t_t/(2L)]^2 \quad (3)$$

Topp et al. [1] found that a single polynomial function described the relationship between volumetric water content, θ_v (m^3 m^{-3}), of four mineral soils and values of ε_a determined in this fashion. Since 1980, other researchers have shown that the relationship between t_t and θ_v is linear for many practical purposes (e.g., [14]).

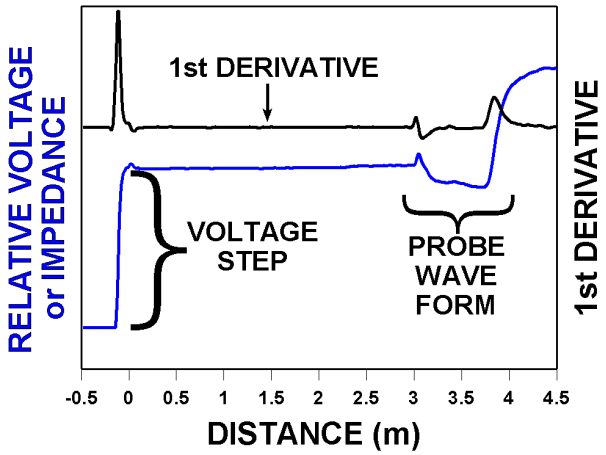

FIG. 1. Plot of wave form and its first derivative from a Tektronix 1502C TDR cable tester set to begin at -0.5 m (inside the cable tester). The voltage step is shown to be injected just before the zero point (BNC connector on instrument front panel). The propagation velocity factor, Vp, was set to 0.67. At 3 m from the instrument there is a TDR probe.

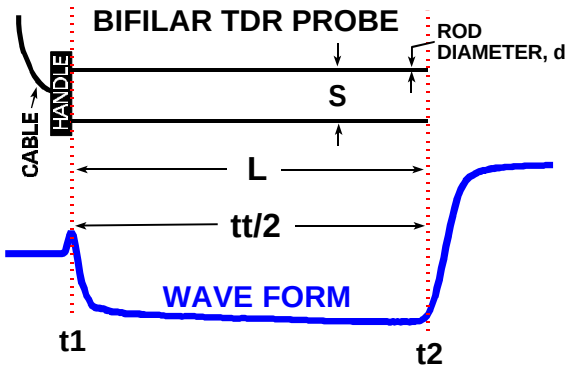

FIG. 2. Schematic of a typical bifilar TDR probe and the corresponding wave form, illustrating probe rod length, L; one way travel time, tt/2; rod spacing, S; and rod diameter, d.

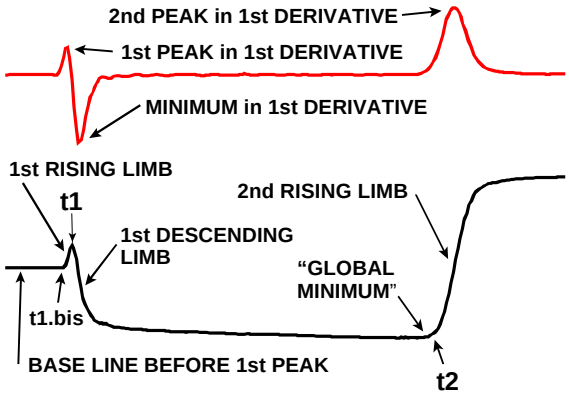

FIG. 3. TDR wave form for a wet sand (bottom) and its first derivative (top) showing features useful for graphical interpretation.

Graphical interpretation depends on the fact that the probe design itself introduces impedance changes in the wave guide. The impedance, Z (Ω), of a transmission line (i.e., wave guide) is

$$Z = Z_0(\varepsilon)^{-0.5} \quad (4)$$

where Z_0 is the characteristic impedance (Ω) of the line (when air fills the space between conductors) and ε is the permittivity of the (homogeneous) medium filling the space between conductors. For our parallel transmission line (the two rods in the soil) the characteristic impedance is a function of the wire diameter, d (m), and spacing, s (m) [15]:

$$Z_0 = 120 \ln\{2s/d + [(s/d)^2 - 1]^{0.5}\} \quad (5)$$

or, if d<<s:

$$Z_0 = 120 \ln(2s/d) \quad (6)$$

For a coaxial transmission line the characteristic impedance is:

$$Z_0 = 60 \ln(D/d) \quad (7)$$

where D and d are the diameters (m) of the outer and inner conductors, respectively.

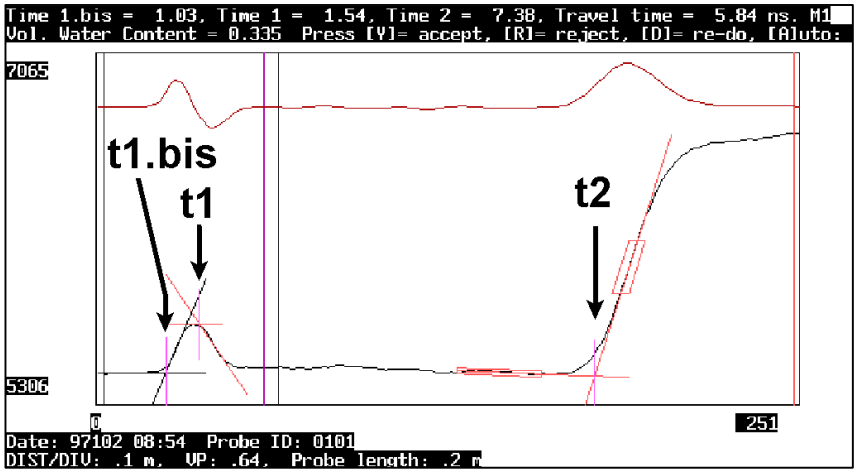

FIG. 4. Example from the TACQ program of graphical interpretation of a wave form from a probe in wet sand. Times t1.bis, t1, and t2 have been labeled. The water content was calculated from Eq. 7 of Topp et al. [1].

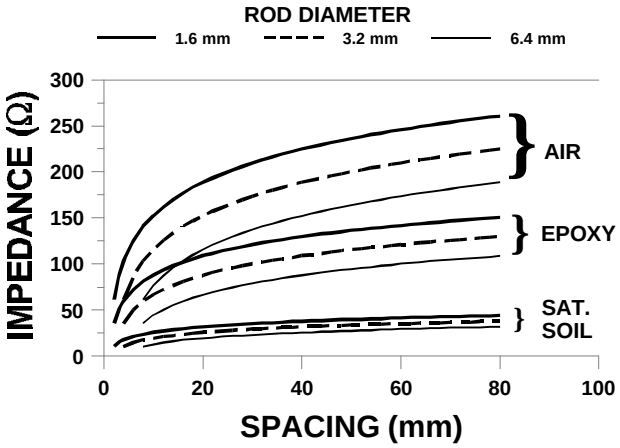

FIG. 5. Influence of rod spacing, rod diameter, and permittivity of the medium on impedance of the wave guide according to Eqs. 4-5. Permittivities are: AIR, unity; EPOXY, close to 3; and SATurated SOIL, approx. 35.

From Eqs. 4 through 7 it is apparent that impedance, Z, increases as wire spacing increases, and decreases as ε (or water content) increases for any probe type (Fig. 5). In the probe handle, the wire spacing increases from that of the coaxial cable to that of the probe rods. The resulting impedance increase causes the wave form level to rise (first rising limb in Fig. 3). If the porous medium in which the probe rods are embedded is wet then the permittivity of that medium will be higher than that of the epoxy probe handle. This causes a decrease in impedance, which results in the descent of the reflected wave form level as the step voltage leaves the handle and enters the rods in the soil (first descending limb, Fig. 3). The combination of impedance increase at the handle and impedance decrease after the handle gives the peak in the wave form. The rod ends are another impedance change in the wave guide, in this case an open circuit. The remaining energy in the voltage step is reflected back at the rod ends, which represent an impedance increase (second rising limb, Fig. 3). As will be discussed later, wave form shapes different from that shown in Figs. 2-4 result from different soil types and conditions (e.g., dry soil, or wet clays). A computer program for automatic TDR data acquisition must be able to acquire the wave form from the probe and correctly interpret it graphically. It should be able to accomplish this despite different cable lengths to the probes, different probe lengths and rod spacings, and different soil conditions.

1.2. **Wave form interpretation**

Topp et al. [11] described a method of interpreting wave forms captured on paper using a chart recorder or by photographing an oscilloscope screen. This analysis involved two graphical algorithms. Algorithm 1 consisted of drawing a horizontal line across the top of the first peak, and drawing a line tangent to the descending limb of the first peak (Fig. 3). The intersection of these lines defined t1 as illustrated in Fig. 4. Algorithm 2 consisted of drawing a horizontal line tangent to the base line between the first peak and second inflection, and drawing a line tangent to the second inflection. The intersection of the latter two lines defined t2. The pulse travel time, in the part of the wave guide that was buried in the soil, was t_t = t2 - t1. Peaks and inflections were identified by eye and no computer code or algorithms were presented.

Later, Baker and Allmaras [6] discussed a computer program for interpretation of wave forms, which followed the ideas of [11], and added the idea of using the first derivative of the wave form to identify important wave form features. The program included the following steps applied to a wave form consisting of 200 data points (Fig. 6):

1) Smooth and differentiate the data [16].
2) Use a loop to search the wave form data for the global minimum, VMIN, and associated time, t2.1.

3) Find the local maximum, V1MAX, and associated time, t1p, in the data between the first point and t2.1. This is the time, t1p, of the first peak.
4) Find the most negative derivative, DMIN, the corresponding time, tDMIN and wave form value, VtDMIN, in a region of 25 points following t1p. The slope of the first descending limb is DMIN.
5) Define a line, with intercept V1MAX and slope of zero, that is horizontal and tangent to the first peak. Define a second line, with slope DMIN and intercept such that it passes through VtDMIN at tDMIN. Solve for the intersection point of the two lines, and the associated time, t1, that corresponds to the point where the rods exit the handle.
6) Find the maximum derivative, D2MAX, in a region of 25 points following VMIN, and associated time t2.2 and wave form value Vt2.2.
7) Define a line tangent to the second inflection with slope D2MAX and passing through Vt2.2 at t2.2. Define a horizontal line tangent to VMIN. Solve for the intersection of these lines to find t2, the time corresponding to the ends of the rods.

The travel time of the pulse through the exposed length of the rods was t_t = t2-t1. While these algorithms worked well for relatively moist soils, there were problems with the absence of DMIN and absence or movement of VMIN and associated times in wave forms for dry, low bulk density soils (see later section on wave forms from dry soils).

Heimovaara and Bouten [7] described a computer program that involved fitting lines to the second inflection and to the base line between t1 and t2. The regions of data points, to which these lines were fit, were determined empirically for a given probe. Also, they recognized that the wave form might not always descend at t1. So, they introduced the concept of fitting lines to the rising limb of the first inflection and to the base line before the first inflection, and using the intersection of these lines to define a time corresponding to the point of separation of the cable conductors. This time is termed t1.bis in this paper, and is illustrated in Figs. 3 and 4. A correction time was added to t1.bis to get t1. This correction time was determined by performing a single measurement in air before probe installation.

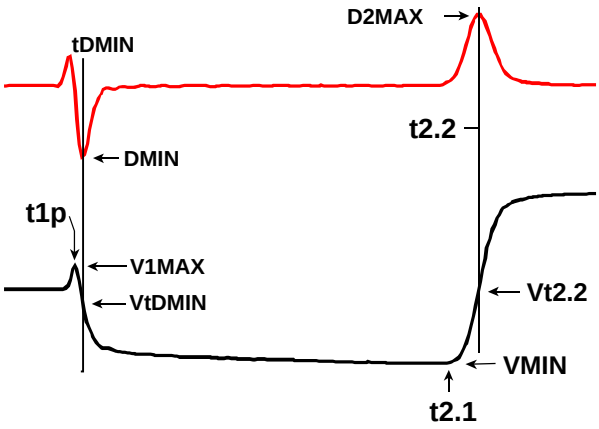

FIG. 6. The TDR wave form (bottom) and its first derivative (top) with features identified by Baker and Allmaras [6] (my nomenclature). Relative wave form heights D2MAX, V1MAX, DMIN, VMIN and Vt2.2 may be considered to be dimensionless. Times t1p, t2.1, t2.2, and VtDMIN are in s.

1.3. **Factors influencing wave form shape**

Many conditions may alter the wave form from the classical forms displayed in Figures 2-4. Early computer algorithms emphasized finding the minimum, VMIN, and its time, t2.1; the second maximum in the first derivative, D2MAX, and its time, t2.2; and the minimum of the first derivative, DMIN, and its time, tDMIN (see Fig. 6). In humid environments, where soils are seldom dry, and are well leached so that bulk electrical conductivity is low, these features are found in almost all wave

forms and can be reliably used as keys for computer analysis. Today, most commonly available TDR probes are connected directly to 50 Ω coaxial cable. For these probes in dry soils, DMIN and the descending limb of the first peak may disappear, making t1 difficult to find. Also, in dry soils, the position of VMIN may change dramatically, moving from the right side to the left side of the wave form between t1 and t2, and causing interpretation problems. Some of the first field probes consisted of two stainless steel rods connected to 200 Ω twin-lead antenna cable. Because impedance in the soil is almost always less than 200 Ω (Fig. 5), there was always a drop in the wave form at the transition from cable to probe rods. This fact tended to favor the use of the earlier algorithms. However, even for these probes, the position of VMIN may be closer to t1 than to t2 in dry soils. In soils with high bulk electrical conductivity the wave form may rise only slowly at the point corresponding to the ends of the rods; making the value of D2MAX so low as to be lost in the noise level of the first derivative. These and other factors influencing wave form shape are discussed below. Later, a suite of algorithms will be presented that allow interpretation of wave forms despite these changes in shape.

1.3.1. *Influence of probe design on wave form shape*

The height of the first peak increases with the separation distance of the rods because the impedance at this point in the wave guide increases with the separation distance (Eq. 5; Fig. 5). The impedance and peak height are inversely proportional to the diameter of the rods. The height is also influenced by the permittivity of the material separating the proximal ends of the probes (in the handle) (Eq. 4). For a handle made of epoxy (ε_a approx. 3), rod diameter of 3.2 mm and spacing of 30 mm, the characteristic impedance increases from 50 ohms in the cable to 152 ohms in the part of the stainless steel wave guide embedded in the handle (Fig. 5). The pulse travel time between t1.bis and t1 increases with the permittivity of the material between the point of splitting the antenna cable and the connections to the rods. It also increases with the separation distance of the rods. Finally, this travel time increases with the distance between the split in the cable and the point of connection to the rods.

Consider an early type of TDR probe consisting of two stainless steel rods buried parallel to one another in the soil, with the proximal ends connected to the split ends of a bifilar antenna cable. Connections were sometimes made using alligator clips, sometimes soldered, and sometimes made by clamping the wire to the rod with a screw. The perpendicular distance between the rods was the separation distance. Typically, the antenna cable would have a characteristic impedance of 200 ohms. A balun would usually be used to connect the antenna cable to the cable tester, in order to match impedances (thus lowering signal loss and distortion) between the antenna cable and the 50 ohm wave guide of the cable tester. For this probe, the connections, and some of the split wire, are separated by the soil between the proximal ends of the rods. There is no first peak for this probe, because the wave form always drops from a level corresponding to the 200 Ω cable to a level corresponding to the impedance at the proximal ends of the rods. But, the point at which the wave form drops is influenced by the water content of the intervening soil (assuming the probe is buried). For dry soil, the impedance may be nearly the same as for epoxy but for wet soil the value of ε_a may approach 35 and the impedance may be 30 ohms or lower (Fig. 5).

Using our probe made with antenna cable and two rods, we can see several reasons why the position of the drop in the wave form and the time of t1 might not be reproducible between probes in the field. The length of cable split may vary, the separation distance at the proximal rod ends may vary (over time even if controlled at installation), and the permittivity of the porous medium separating the two wires of the cable may vary in time and space between the cable split and the point of connection to the rods. If the rods are installed vertically, and the point of connection is at the soil surface, the split cable may be separated by air; whereas if the probe is installed deeper in the soil, the split cable will be separated (along at least some of its length) by soil that varies in permittivity as it wets and drys.

For these reasons, the TDR probes commercially available today are invariably made with the split in the cable (usually coaxial cable), and the connections to the rods, fixed in some sort of rigid configuration, usually called the handle, which is encased in a material of consistent and constant permittivity. The handle may be made of epoxy resin, delrin, polymethyl methacrylate (acrylic), RTV

silicone or some other plastic and may contain metal for shielding or connection of rods. These handles share the properties of a fixed separation distance, fixed permittivity of the material separating the conductors of the wave guide in the handle (with some minor temperature variations), fixed distance between the cable split and the point of connection to the rods, and fixed distance between the point of connection at the proximal ends of the rods and the point at which the rods exit the handle and enter the soil. Such handles provide optimal conditions for reliable algorithms determining t1.bis and t1, and the rest of this discussion will assume such a handle.

It has been argued (e.g., [17]) that in order to match impedances (thus lowering signal loss and distortion) between the coaxial cable and the two rods in a bifilar probe, a balun should be used at the point of connection. Also, the balun should serve to convert the unbalanced signal in the coaxial cable (where the inner conductor carries the wave form and the outer conductor remains at virtual ground) to a balanced signal in the two rods (where both conductors carry the wave form). The argument states that, absent a balun, the unbalanced signal will tend to balance as it travels down the rods, eventually becoming closely balanced at some point along the rods. But, between the handle and that point, the signal reflections will be distorted due to the partial imbalance. If the rods are very short, the distorted part of the wave form may interfere with the second inflection. The trifilar probe responds to this concern by providing a wave guide that is geometrically more similar to a coaxial wave guide [18]. Measurements by Zegelin et al. [18] show only minor differences in wave form shape between trifilar and coaxial wave guides.

1.3.2. *Influence of dry soil on wave form shape*

As the soil dries, the first descending limb (Fig. 3) becomes less steep. Because dry soil has about the same permittivity as the plastic materials used in most probe handles, there may be little or no impedance change between the wave guide in the handle and in the soil. Indeed, if the soil is both dry and of low bulk density, the impedance of the wave guide may actually increase in the soil compared with the handle. Both conditions cause the first descending limb to be almost absent, and may cause the wave form level to rise between t1 and t2 (between vertical lines in Fig. 7), so that VMIN is located close to t1. This renders ineffective both algorithm 1 of Topp et al. [11] and the corresponding methods of Baker and Allmaras [6]. Dry soils of low bulk density are usually found close to the surface. This is where the TDR method enjoys its greatest advantage compared with neutron scattering. Thus, it is imperative that the method be usable in such soils. For dry soil, the second inflection, caused by the distal ends of the rods, is invariably steep and high, making it easy to find by searching for D2MAX. However, at the same time, the global minimum may not occur after t1, or the position of the local minimum may shift from just before the second inflection to a point just after the first peak, or to any intermediate position. This causes variations in the intersection of the two lines (horizontal tangent to global minimum and tangent to second inflection) that have no relation to the travel time, t_t.

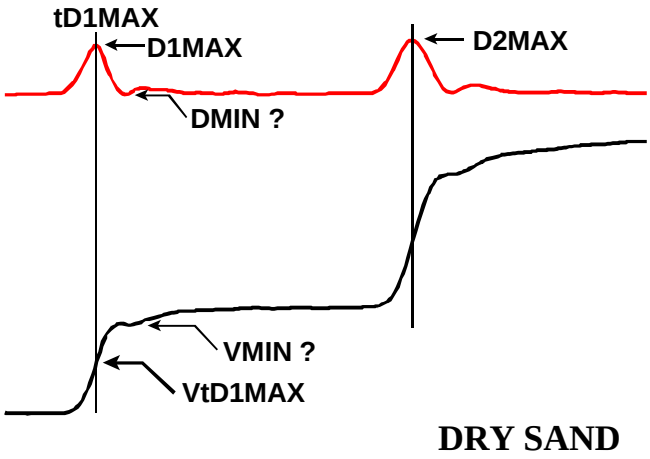

FIG. 7. Influence of dry soil on wave form shape, illustrating difficulty of finding DMIN and VMIN.

Another phenomenon sometimes found in low bulk density soils is the double peak. This may be due to compression of a thin layer of soil next to the handle as the probe was inserted into the soil at installation time. This higher bulk density soil will exhibit a lower impedance due both to lower porosity (air has a permittivity of 1, soil minerals have permittivities of 3 to 5, so denser soils have higher apparent permittivities) and to correspondingly higher water content (at equilibrium with surrounding soil), and will cause the dip in the wave form after the handle. As the pulse enters less compressed soil it encounters a higher impedance and the reflected wave form rises, only to lower again as the pulse travels further down the rods (if the soil is at all moist). It is important to have an algorithm to discriminate between these peaks.

1.3.3. *Influence of bulk electrical conductivity on wave form shape*

As the bulk electrical conductivity (BEC) of the soil increases, the impedance of the wave guide in the soil decreases due to the lowering of the resistance component of impedance. Also, there is a lowering of signal voltage along the length of the rods due to conduction through the soil. This causes the wave form level after the first peak to decline relative to that for a soil of lower BEC. It also lowers the slope, D2MAX, of the second rising limb [19] and the final height to which the wave form rises after the second inflection. The latter fact has been used successfully to find the BEC of soils, e.g., [2, 5, 20].

However, these effects can make it difficult to reliably find the second rising limb by searching for D2MAX. Smoothing of the wave form and its first derivative can make the determination of D2MAX more reliable by reducing the relative height of peaks in the first derivative that are caused by random noise in the wave form. However, in the case of a very weak second rising limb, the peak in the first derivative can be so spread out that the apparent position of the second rising limb, deduced from the position of D2MAX, is not consistent (Fig. 8). Fortunately, in these cases the high BEC guarantees that the wave form will slope downward between t1 and t2, in turn guaranteeing that the position of VMIN is always just before the second rising limb. In this situation, VMIN can be used reliably as the key to an algorithm used to find t2.

Unfortunately, increased soil salinity is only one source of increase in BEC. Another source of BEC is the conductivity arising from certain clays, especially clays with high CEC. These are often expanding lattice clays containing cations entrapped between clay layers. When such soils are dry they exhibit low BEC, probably due to the contracted nature of the clay micelles, the discontinuous water films on soil particles, and the resulting low mobility of cations. As these soils wet, their BEC increases as shown in Fig. 9 for an expansive Pullman clay loam with mixed mineralogy at Bushland, TX. The effects are apparent as a lowering of the second inflection and final wave form height as these soils wet. Although the problems posed by this phenomenon, vis-a-vis the finding of t2, can usually be solved, the implications for relating TDR wave forms to soil salinity cannot be ignored.

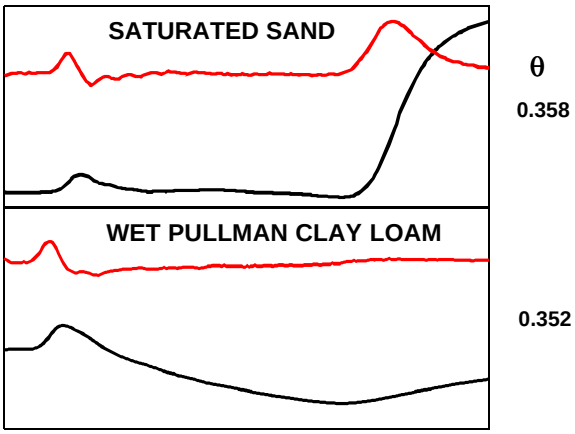

FIG. 8. Wave forms and their first derivatives (top lines in each plot) for two soils showing the lack of a distinct peak in the first derivative corresponding to the second rising limb of the wave form for the wet clay loam. Although the sand is slightly wetter, there is a distinct peak in the derivative useful for finding t2.

Furthermore, this phenomenon has implications for the application of frequency domain (FD) probes to water content determination in these soils, similar to the implications and reported problems related to salinity effects on water content determination by FD probes. A frequency domain probe relies upon the change in frequency of an oscillator circuit caused by the change in permittivity of the soil around the probe. For the oscillator to change states, the reflected voltage must reach the set point voltage of the oscillator at which time the oscillator changes states and drives the wave guide to the opposite polarity. The time it takes for the reflected voltage to reach the set point is determined not only by the travel time to t2 but by the additional time between t2 and the time at which the second rising limb rises to the set point. Thus, the frequency of oscillation is dependent not only on t2 or t2-t1 but on the BEC of the medium. Because the BEC may be changed by salinity changes, clay content changes, and/or water content changes in a clayey or saline soil it is obvious that calibration of an FD probe for routine field use, where these factors may change in time and space, is problematic.

Figure 9 illustrates that the width of the wave form increases as the soil becomes wetter. This has implications for correct positioning of the wave form in the window and choice of window width settings Vp and Dist/Div, as will be discussed later. Not all clay soils show increases in BEC with water content as shown in Fig. 10 for a Cecil clay of kaolinitic mineralogy from Watkinsville, GA. Figures 9 and 10 both illustrate the loss of the first descending limb and VMIN as the soil dries.

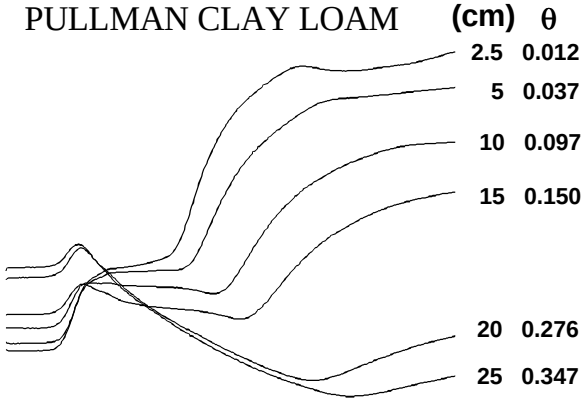

FIG. 9. Effect of soil water content (q, m^3 m^{-3}) on the bulk electrical conductivity of a non-saline soil at several depths (cm) in the silty clay loam A horizon (2.5 to 15 cm) and the clay B horizon (20 and 25 cm).

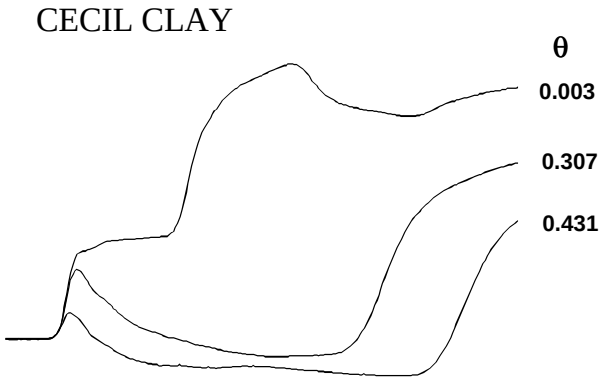

FIG. 10. Effect of soil water content (q, m^3 m^{-3}) on the bulk electrical conductivity of a non-saline Cecil clay (kaolinitic).

1.3.4. *Influence of cable length on wave form shape*

As the pulse moves down the cable to the probe, its higher frequency components are selectively attenuated because the cable acts as a low pass filter. This means that the longer the cable, the slower the rise time of the pulse at the probe, and the less steep the rising and descending limbs of the inflections caused by probe handle and end of rods [19, 21]. If the wave form is correctly interpreted, then the travel time, t_t, should be constant despite cable length. However, if the probe is short enough, the descending limb of the first peak will intersect the rising limb of the second inflection causing the travel time to be incorrect. The longer the cable, the lower the slope of the descending limb and the longer the probe must be to avoid this problem. Since the slope of the descending limb also decreases with increasing BEC of the soil, a probe length adequate for a given cable length is difficult to predict. Another problem associated with long cable lengths is the loss of the first peak altogether.

1.4. **Setting window width**

To this date, there are no reports describing a method for setting the TDR window width that allows for reproducible and consistent computerized finding of t_t. Yet, positioning has a direct effect on whether enough data are present to reliably fit lines to various portions of the wave form. Consider wave forms similar to those in Figs. 2-4. Because the data are digital representations of an analog phenomenon there are only a fixed number of data pairs of voltage and time representing a screen of data. For instance, for the Tektronix model 1502B/C cable testers there are 251 data pairs. For Fig. 2 there were only four data pairs in the first rising limb, 12 data pairs in the first descending limb, and about 25 data pairs in the second rising limb. If similar wave forms were compressed horizontally, even by 50%, it would be difficult to find enough data points to reliably fit tangent lines to key parts of the wave forms. Thus, it is best to have the wave form occupy as much of the screen as possible. This is easily accomplished using the distance per division, Dist/Div, and propagation velocity factor, Vp, settings of the cable tester. However, the width of the wave form increases with soil water content, and unless the cable tester is set when the water content is at saturation the wave form may widen enough, with increasing water content, that the second rising limb can no longer be seen on the screen. Figures 9 and 10 illustrate this. If the wave form width had been set to occupy the full screen for dry soil, the wave form for wet soil would be too wide for the second rising limb to appear on the screen.

Fortunately, if we have a good idea of what the saturated water content would be for a given soil, we can compute the desired screen width in nanoseconds as follows. First, compute the apparent permittivity from Eq. 8 [1] and the saturated water content θ_s ($m^3\ m^{-3}$)

$$\varepsilon_a = 3.03 + 9.3\ \theta_s + 146\ \theta_s^2 - 76.7\ \theta_s^3 \qquad (8)$$

The saturated water content can be estimated from the soil dry bulk density, ρ_b (Mg m^{-3}). Simply calculate the total soil porosity ($m^3\ m^{-3}$), $f = 1 - \rho_b/\rho_p$, where ρ_p is the particle density (assumed equal to 2.65 Mg m^{-3}); and assume that all air is displaced when the soil is saturated so that $\theta_s = f$.

Second, re-arrange Eq. 1 to calculate the velocity, v, of the signal in the wave guide

$$v = c_o(\varepsilon_a \mu)^{-0.5} \qquad (9)$$

Then calculate the travel time over the length of the probe from

$$t = L/v \qquad (10)$$

where L is the probe length. Adding additional time for the base line before the first peak and for the second rising limb after t2, we have the time that we wish to have represented by the full screen width. Then we have only to find a combination of Dist/Div and Vp settings that results in a full scale horizontal axis at least equal to this time. Experience shows that it is best to have at least one tenth of

the screen width (one division) between the left-hand side of the screen and the first peak, in order to reliably fit the base line. Also, it is best to have at least 0.2 of the screen width between t2 and the right hand side of the screen to reliably fit the tangent to the second rising limb. A computer algorithm for finding appropriate combinations of Dist/Div and Vp, given the soil's saturated water content and the probe length, is given in Appendix A. Example results for several probe lengths and saturated water contents are given in Table I. These are for the Tektronix 1502B or 1502C cable testers, which allow variation of Vp settings in hundredths.

For the older Tektronix model 1502 cable tester, the Vp setting has much less flexibility. There are three buttons for Vp. Pressing Solid PTFE gives a Vp of 0.70; pressing Solid POLY gives a Vp of 0.66; and pressing OTHER allows the Vp to be adjusted from 0.55 to 0.99 by turning the VAR screw. When all three buttons are out the Vp is 0.99; or, when the OTHER button is pressed in and the VAR screw is turned all the way clockwise, the Vp is 0.99. Unfortunately, there is no simple way to know the exact Vp value that is set with the VAR screw, so the user is left with just three usable Vp settings, 0.66, 0.70, and 0.99. If the Tektronix 1502 is selected in Software Setup in TACQ, then pressing D for defaults will, in addition to allowing the user to set the Vp and Dist/Div settings, give two recommendations for Dist/Div (using the Vp value chosen by the user). The first recommendation will show a negative percent error, and the second will show a positive percent error. These are the percentage differences from the optimum screen width in ns. If the negative percent error is small, then the user may be able to use the corresponding Dist/Div recommendation. Otherwise, the user should use the Dist/Div recommendation that gives a positive percent error. This will result in a screen width in ns that is wider than absolutely necessary, but that will ensure that the second rising limb of the wave form is not lost off the right side of the screen when the soil becomes saturated. The user should use Vp values of 0.66, 0.70, and 0.99 and see which gives the smallest percent error. Tables II and III give some possible combinations of probe length and Dist/Div, and associated errors as a percentage of the optimum screen width in ns for Vp values of 0.99 and 0.70, respectively. These tables are given in units of feet because most of the model 1502 cable testers were built at the factory to use English units.

It is obvious that, for some combinations of probe length and saturated water content, there is no combination of Dist/Div and Vp settings, possible with the push buttons on the Tektronix 1502 cable tester, that comes close to providing an optimum screen width. This does not necessarily mean that good data can not be obtained, but it does mean that the user may want to choose probe lengths that lend themselves more easily to optimization of this sort.

TABLE I. OPTIMUM PROPAGATION VELOCITY FACTOR (VP) AND DISTANCE PER DIVISION (Dist/Div) SETTINGS AND RESULTING SCREEN WIDTHS IN NS FOR SEVERAL COMBINATIONS OF PROBE LENGTH AND SATURATED WATER CONTENT (θ_s). SETTINGS GIVE SCREEN WIDTHS WITHIN 2% OF THOSE CALCULATED USING THE ASSUMPTIONS IN THE PRECEEDING PARAGRAPH.

	$\theta_s = 0.5$			$\theta_s = 0.4$			$\theta_s = 0.3$		
Probe Length (m)	Vp	Dist/Div (m)	Screen Width (ns)	Vp	Dist/Div (m)	Screen Width (ns)	Vp	Dist/Div (m)	Screen Width (ns)
0.05	0.59	0.025	1.40	0.69	0.025	1.20	0.85	0.025	0.98
0.10	0.59	0.05	2.80	0.69	0.05	2.39	0.42	0.025	1.96
0.15	0.39	0.05	4.20	0.46	0.05	3.59	0.56	0.05	2.94
0.20	0.59	0.10	5.61	0.69	0.10	4.78	0.42	0.05	3.92
0.30	0.39	0.10	8.41	0.46	0.10	7.18	0.56	0.10	5.87

TABLE II. DISTANCE PER DIVISION (Dist/Div) SETTINGS, AND ASSOCIATED ERRORS COMPARED WITH OPTIMUM SCREEN WIDTH, FOR VP OF 0.99 AND FOR A RANGE OF SATURATED WATER CONTENTS (θ_s) AND PROBE LENGTHS. FOR A CABLE TESTER SET FOR UNITS OF FEET.

	$\theta_s = 0.5$		$\theta_s = 0.4$		$\theta_s = 0.3$	
Probe Length (m)	Dist/Div (ft)	Percent Error	Dist/Div (ft)	Percent Error	Dist/Div (ft)	Percent Error
0.05	0.1	-27	0.1	-14	---	---
0.05	0.2	47	0.2	72	0.1	5
0.10	0.2	-27	0.2	-14	0.1	-48
0.10	0.5	83	0.5	115	0.2	5
0.15	0.2	-51	0.2	-43	0.2	-30
0.15	0.5	22	0.5	43	0.5	75
0.20	0.5	-8	0.2	-57	0.2	-48
0.20	1.0	83	0.5	7	0.5	31
0.30	0.5	-39	0.5	-28	0.5	-13
0.30	1.0	22	1.0	43	1.0	75

TABLE III. DISTANCE PER DIVISION (Dist/Div) SETTINGS, AND ASSOCIATED ERRORS COMPARED WITH OPTIMUM SCREEN WIDTH, FOR VP OF 0.70 AND FOR A RANGE OF SATURATED WATER CONTENTS (θ_s) AND PROBE LENGTHS. FOR A CABLE TESTER SET FOR UNITS OF FEET.

	$\theta_s = 0.5$		$\theta_s = 0.4$		$\theta_s = 0.3$	
Probe Length (m)	Dist/Div (ft)	Percent Error	Dist/Div (ft)	Percent Error	Dist/Div (ft)	Percent Error
0.05	---	---	---	---	---	---
0.05	0.1	4	0.1	21	0.1	48
0.10	0.1	-48	0.1	-39	0.1	-26
0.10	0.2	4	0.2	21	0.2	48
0.15	0.2	-31	0.2	-19	0.2	-1
0.15	0.5	73	0.5	102	0.5	147
0.20	0.2	-48	0.2	-39	0.2	-26
0.20	0.5	30	0.5	52	0.5	85
0.30	0.5	-14	0.2	-60	0.2	-51
0.30	1.0	73	0.5	1	0.5	24

1.5. **Algorithms for wave form interpretation**

This section briefly describes algorithms used by TACQ for automatic graphical interpretation of a wide variety of wave forms. The user may choose from several methods described in the literature or use methods available only in TACQ. These methods assume wave forms correctly positioned in the instrument window as described in the preceding section. Features of the wave form and its first derivative, discussed below, are defined in Figures 3, 10, and 11. Pre-defined, recommended values of all user choices are stored in TACQ. The TACQ program and documentation in Adobe PDF format are free for download from the Internet at http://www.cprl.ars.usda.gov/programs/.

1.5.1. *Wave form smoothing*

Following the method of Baker and Allmaras [6], wave forms are smoothed using the Savitsky-Golay procedure [22]. The user may choose any degree of smoothing from none to a 21-point smooth. To provide a symmetrical smooth, only odd numbers of points are allowed. Derivative smoothing may vary from none to a 19-point smooth. Derivative smoothing must be over a number of points at least two lower than the number chosen for wave form smoothing. The user should specify only enough smoothing to reduce extraneous peaks in the first derivative. Excessive smoothing can cause errors, most particularly loss of sharp wave form features such as the first peak. The default setting for smoothing is 9 points on the wave form and 3 points on the first derivative.

1.5.2. *Circumscribing wave form interpretation*

In order to avoid dealing with sudden drops or rises in level that may occur at the beginning or end of the wave form (usually only seen with the older analog model 1502 cable tester), the user may set any number of points not to be used in wave form interpretation at either end of the wave form. Vertical lines on the screen show the parts of the wave form thus excluded. The number of excluded points for either end may be set by entering a number or by moving the lines interactively using the cursor keys.

Also, the user may exclude data in the right hand side of the wave form from being used to find the first peaks in the wave form and first derivative. This excludes the second peak in the first derivative from consideration for finding time 1 and eliminates confusion between the first and second rising limbs. Correspondingly, the user may exclude a portion of the left hand side of the wave form from consideration when determining the location of the second rising limb. Again, these limits may be set by entering a number or by using the cursor keys to move the vertical lines that represent the limits on the computer screen. Table IV summarizes the user-set limits.

TABLE IV. USER SET LIMITS ON DATA SEARCHED FOR WAVE FORM FEATURES. RELATIVE TIMES ARE DIMENSIONLESS.

Limit Name	Description
StartPt	Relative time before which to exclude data from examination.
EndPt	Relative time after which to exclude data from examination.
D2Lim	Relative time at which to begin search for second maximum in the first derivative. Search ends at EndPt.
D1Lim	The data between StartPt and the relative time D1Lim are searched for the first peak in the first derivative, D1MAX.
SafetyLim	If t1 is less than this relative time then zeros are written to the output.
t1Swath	Number of data points after tD1MAX to use when searching for V1MAX.

1.5.3. *Choosing wave form interpretation methods*

Time 2.2 and tangent to rising limb. For finding the center of the second rising limb (t2.2), the user may choose to use: i) only a global minimum method (i.e. find VMIN and t2.1, and set t2.2 as t2.1 plus a user-set number of points), ii) only a method that finds D2MAX and associated time t2.2, or iii) an automatic method that uses the global minimum method if the value of D2MAX is below a user set threshold, D2Thresh, and that uses the time of D2MAX otherwise. The third method is recommended. The global minimum method for t2 is similar to that of Baker and Allmaras [6], except that the search for VMIN is conducted in the data between t1p and EndPt rather than over all the data. Regardless of the method for finding t2.2, the line tangent to the second rising limb is found by linear regression on a swath of points around t2.2 (user chosen swath width).

Time 2.1 and tangent to VMIN or fit to base line. The user may choose how to fit the "horizontal" intersecting line that partially defines t2. The line is either: i) a horizontal line passing through the wave form at t2.1, or ii) a line fit by regression to a swath of points just prior to t2.1 (user chosen swath width). The second method is recommended. Travel times found with it are less susceptible to temperature induced errors [23]. If the horizontal tangent method is chosen, the program will examine the slope of a line fitted to the swath of points; and, if the slope is positive, the program will use the fitted line rather than the horizontal tangent. This avoids improper interpretation of wave forms from dry soils for which VMIN may be located closer to t1 than t2 and the wave form slope may be upward between t1 and t2.

Time 1. For finding t1, the user may choose between two methods, M1 or M2. Method M1 is similar to that of Baker and Allmaras [6], and finds t1p by searching for V1MAX and DMIN. But, it starts the search from the time of D1MAX. If it fails to find V1MAX and D1MAX, it assigns values as explained in Appendix B. Method M2 finds D1MAX and fits a line tangent to the first rising limb. It also fits a horizontal line tangent to the baseline before the first rising limb and solves the intersection for t1.bis. Method M2 then adds a user set time, t_C, to t1.bis to get t1. The time t_C = t1 - t1.bis is found by measurements on probes installed in wet soil using method M1. This is different from the method proposed by Heimovaara and Bouten [7] involving a single measurement in air. Method M2 is recommended.

Appendix B describes the steps the program takes to find times t1.bis, t1, and t2.

1.6. **Measuring bulk electrical conductivity**

Several papers discuss how to calculate the bulk electrical conductivity (BEC) of a porous medium from the relative wave form heights measured at several points along the TDR wave guide (see, among others, [2, 3, 4, 5, 17, 18, 20, 24, 25, 26]). Paper [20] is notable for simplicity, clarity, and a method for probe- and soil-specific BEC calibration. The measurement of BEC is discussed here in order to lend insight into the effect of BEC on the TDR wave form and its interpretation. There are six points along the wave guide where these heights are measured in the various studies cited. No one method of calculating BEC uses all six, but they are discussed here for completeness. The wave form heights at these points may be designated V_{01}, V_{min}, V_{02}, V_F, V_I, and V_R (all dimensionless), which are defined for a Tektronix model 1502B/C cable tester as follows (Fig. 11):

V_{O1} The voltage of the wave form before the first peak, i.e., the pre-incident pulse height. This is taken from the regular wave form that the user sets up for determination of water content. If the first peak is set to occur just at or after the first vertical division on the screen, then this value of V_O will be the average of about 15 to 25 points. The actual number of points depends on what the program determines to be the flat part of the wave form before the first peak. This value is determined by the program for the use of those who might want to use a particular method cited in a paper. This value is somewhat noisier than the second value of V_O (see below). The second value of V_O is preferred for BEC calculations.

V_{MIN} Again, this value is taken from the regular wave form that the user set up for determination of water content. It is the voltage of the minimum of the wave form between the first peak caused by the probe handle and the final reflection caused by the ends of the rods. Some persons have used this value for BEC calculations, but there are better methods now. It is output by TACQ for compatibility with older techniques. The value of V_{MIN} is more noisy than the others because it is a single point value, not an average. Applying more wave form smoothing will reduce the noise somewhat; but the extra smoothing may cause problems with wave form interpretation for water content. This is the only value that is taken from the smoothed wave form.

V_{O2} The second value of V_O is acquired by first moving the 'regular' wave form view one tenth of its length to the left (one Dist/Div to the left), and then taking the average of the first 25 data points. These data are the first 25 data to the left of the beginning of the regular wave form that the user set up for determination of water content. Normally the two values of V_O should be the same, but the first value is slightly more noisy because of the possibility that some data from the initial part of the rise of the first peak may inadvertently be included in the averaging.

V_F The voltage of the wave form at great distance (final voltage). To find this, the program sets Dist/Div to 1 m or 2 feet, sets the wave form to start at 599 m or 1980 feet (maximum distance setting on the cable tester), and then takes the mean of the last 50 data points.

V_I The initial voltage of the wave form before the voltage pulse is injected. This is virtual zero for the TDR system and all other voltages may be normalized by subtracting V_I from them. The program sets Dist/Div to 0.1 m or 0.5 foot, sets the start of the wave form to -0.51 m or -2 feet, and takes the mean of the first 25 data points. The negative distance setting means that the wave form that we are looking at here is inside the cable tester, before the BNC connector on the front panel and before the pulse is injected (see Fig. 1).

V_R This is called the relative voltage and is used in the paper by Baker et al. [27]. It is determined from the same wave form as for V_I but is the mean of the last 25 data points of the wave form. This is in the cable outside the cable tester and after the pulse is injected. Note that the values of V_R, V_{O1}, and V_{O2} are all about the same, differing only due to changes in impedance due to cable resistance, cable type before and after the multiplexer (if there is one), noise, etc. In general, V_R tends to be slightly smaller than either V_O value.

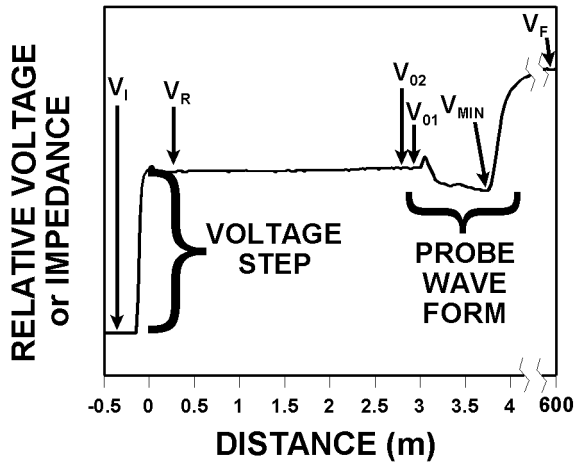

FIG. 11. Wave form showing the relative voltages or impedances measured for determination of BEC.

The measured load impedance, Z_L, (ohms) is used in most methods of calculating bulk electrical conductivity:

$$Z_L = Z_{REF}(1 + \rho)/(1 - \rho) \quad (11)$$

where Z_{REF} is the output impedance of the cable tester (50 ohms), and where the dimensionless ratio ρ is

$$\rho = E-/E+ \quad (12)$$

where the dimensionless potential difference E- is

$$E- = V_F - V_{O2} \quad (13)$$

And the dimensionless potential difference E+ is

$$E+ = V_{O2} - V_I \quad (14)$$

For most methods only V_{O2}, V_I, and V_F are needed. Because BEC calculation from TDR data is still a subject of active research, the other values are included for backward compatibility with methods of calculating BEC reported in the literature.

1.7 **General remarks**

The TDR method for soil water content measurement is a widely applicable method that may be used for unattended, automated data collection. But, obtaining precision and accuracy in automated measurement is very much dependent on the robustness of wave form interpretation methods used in the software or firmware of the data logging equipment. Interpretation methods presented here allow TDR to be used for a wide variety of agricultural soils that are primarily mineral in nature. And, for these soils, TDR is the only method for which a nearly universal calibration exists [1]. Soils high in swelling clays may exhibit a bulk electrical conductivity that is not related to soil solution salinity, but which conducts and weakens the TDR signal and limits both the usefulness of TDR and the length of probes. But, TDR may be used easily in other clay soils such as those high in kaolinitic clay, which affect the signal no more than does sand. Commonly used TDR probes are bifilar or trifilar configurations that must be inserted into the soil or buried, limiting their use to near the surface in soils whose structure is disturbed by digging of pits. Probe length is limited both by conduction losses and by the difficulty of inserting probes into soil. Thus, common probe lengths are in the range of 10 to 50 cm. In deep sands, probes may be installed much deeper, up to 3 m in at least one case; and probe length may be as long as 1.5 m or more in sand if the soil water is not saline. Probes using shorting diodes exist in versions as long as 1.5 m or more for use in most soils. Shorting the diodes and measuring signal differences enhances the signal-to-noise ratio in these probes, and thus the length possible. But, there is no soil between the two sides of the wave guide in these probes and they are sensitive to only a small volume of soil outside the probe. Small measurement volume is both a weakness and strength of TDR. For bifilar and trifilar probes, most of the TDR signal is concentrated in a volume that extends about 2 cm above and below the plane of the rods, and about 2 cm outside the rods. However, the capacity to custom tailor measurement volume by changing rod length and spacing is a major advantage of TDR.

2. NEUTRON SCATTERING

Neutron scattering (NS) was first successfully used for measuring soil water content in the 1950's [28]. Since then NS gauges have improved in portability, programmability, weight and size. The advent of more efficient detectors resulted in the use of smaller and thus safer radioactive sources. The precision of measurements possible with NS has always been high and satisfactory for many soil water investigations (standard error <0.01 $m^3 m^{-3}$, [29, 30]). However, safety regulations requiring costly licensing and training of users, and considerable (and apparently growing) paperwork cause the NS method to remain expensive and difficult or impossible to use in some situations, particularly unattended monitoring. Storage and disposal of the radioactive sources in these gauges is also increasingly expensive. The theory of operation of NS gauges and field calibration methods are described in several publications including [30] and [31]. Careful calibration and use remain essential to accurate soil water measurement with NS gauges. The following discussion will concentrate on some calibration methods explored in the 1990s and recommendations for calibration and use.

2.1. **Calibration**

Stone et al. [32] conducted the ASCE (American Society of Civil Engineers) Neutron Probe Calibration Study on three agricultural soils, Millville silt loam, Nibley silty clay loam, and Kidman sandy loam. Sub-studies were done on methods of bulk density measurement, effects of the geometry of source and detector tube (source at bottom of detector, or source centered around detector), and effects of access tube material (aluminum, steel or polyvinyl chloride plastic). No attempt was made to produce calibrations for different soil horizons, probably because sample numbers were inadequate (they ranged from six to eighteen for the entire profile). Three access tubes were installed in a wet site and three in a dry site for each soil, with 10 cm of the tube protruding above ground level. Sampling depths were at 15 cm below ground surface and in 15-cm increments below that to 150-cm depth. Shield counts, used to calculate count ratios, were taken with the gauges resting on the top of an access tube at 1.5 m above the soil surface. Calibration equations were calculated by linear regression analysis of measured volumetric water content vs. count ratios.

A probe with the source centered around the detector tube (model 3223, Troxler Electronics Inc., Research Triangle Park, NC) showed greater sensitivity to water content than the probe with the source at the bottom of the detector (model 503DR, Campbell Pacific Nuclear (CPN) International, Martinez, CA) [33]. The two probes were equally sensitive to proximity to the surface. The centered detector-source probe showed slightly better resolution of vertical changes in moisture content and of a cavity placed in the soil adjacent to the access tube. Both probes were sensitive to placement above the bottom of the augered access hole. Changes were 1.64 standard deviation (SD) for the Troxler and 1.19 SD for the CPN, from readings with the probes about 10 mm above the bottom of the hole, when the hole was augered another 15 cm deeper and readings were taken at the same depth. This suggests that calibration efforts should ensure that the augered hole extends well beyond the lowest depth of reading. Despite the greater sensitivity of the Troxler probe, there was no significant difference in the precision of calibration curves developed for the two brands of gauges [34]. Standard errors of estimate ranged from 0.0068 to 0.0193 $m^3 m^{-3}$ for CPN gauges and from 0.0056 to 0.0197 $m^3 m^{-3}$ for Troxler gauges [35].

Access tube materials affected the calibration equation slope a great deal, but affected the intercept only slightly. Both brands of gauge were more sensitive to water content when used with aluminum tubing and least sensitive when used with polyvinyl chloride (PVC) tubing. Sensitivity with steel tubing was in between that for Al and PVC tubing [34]. Calibration equation standard errors of estimate ranged from 0.0056 to 0.0147 $m^3 m^{-3}$ for Al access tubes and from 0.0111 to 0.0193 $m^3 m^{-3}$ for PVC access tubes, indicating a slight reduction in precision of calibration when using PVC tubes.

Three soil sampling methods for neutron probe calibration that do not destroy the site were compared by Allen et al. [35] and Dickey et al. [36]. Two were down-hole methods for which samplers were pushed into the soil at the bottom of an augered hole to take fixed volumetric samples. Of these, the SCS Madera sampler, with a 60 cm^3 sample volume, resulted in better calibrations (lower

standard error of estimate) than the Utah State University sampler that had a smaller volume of 15 cm^3. The third method, involving a Giddings coring tube, produced the smallest calibration error estimates. With this method the coring tube was inserted by a hydraulic coring machine (Giddings Machine Co., Fort Collins, CO) and the soil core was pushed out of the tube onto a tray where it was cut into sections of known length, which were placed in soil cans. Volume of each sample was calculated from the inside diameter of the coring tube cutting edge and the sample length. Use of the Giddings coring tube did result in compaction of the soil around the hole in which the access tube was subsequently installed, and this caused the calibration slope to change. Thus, although the calibration error estimate was smaller with this method of sampling, the calibration probably did not provide an accurate representation of the field soil water content. An added disadvantage of the Giddings coring method is that it requires an expensive tractor or trailer mounted hydraulic coring machine, which may be difficult to operate in the field. Two types of driven, ring samplers were also tested [36]. These required destruction of the site because holes had to be dug to take samples at every depth. These samplers were closed at the ends causing some samples to be compacted. Calibration equation error estimates were higher with data from the ring samplers.

Evett and Steiner [37] calibrated three Troxler and three CPN gauges in an Amarillo fine sandy loam with a sandy clay loam B horizon between 30 and 110 cm depth and a calcic horizon (Btk) below 110 cm. They used schedule 10, galvanized steel electromechanical tubing for access tubes, which were installed by pushing them into hand-augered holes of the same diameter as the outside diameter of the tube. A dry soil site was found in a fallow field and a wet site was created adjacent to it by berming an area and ponding water on it until the soil was wetted to 2-m depth. Three access tubes were installed in each site. The wetted soil was allowed to drain to field capacity (43 h) before sampling began, and sampling at the wet site was conducted in one 11 h period to minimize changes in soil water content due to drainage.

Shield counts were taken before and after counts in the access tubes, and each standard count used for calculating count ratios was the average of at least six shield counts. The CPN gauges reported a χ ratio for each standard count. The χ ratio is a statistic that is valuable for screening shield counts. It is the ratio of the standard deviation of counts to the square root of the mean count. Because the count of thermalized neutrons behaves as a Poisson distribution, the χ ratio should equal unity. Shield counts for which the χ ratio was <0.9 or >1.1 were eliminated from consideration. In order to avoid any influence of soil moisture on the count, shield counts were taken with the gauge resting on a stand 82 cm above the soil surface. Counts in the access tubes were also taken with the gauge resting on the stand. The stand was designed to fit over the access tube and rest on the soil surface around the tube. This procedure provided two benefits. First, the cable stops, used to position the probe at each sampling depth in the tube, were fixed on the cable such that the first reading was at 10 cm below the bottom of the stand, and thus 10 cm below the soil surface. With the stand resting on the soil surface, readings were always at the correct depth regardless of the height of an individual access tube above the soil surface. Second, because the probe and shield were separated by at least 90 cm, for the shallow 10-cm reading there was no question of the count being influenced by the gauge shield, as has been suggested by Stone et al. [33]. Neutron probe readings (1 min counts) were made at 10-cm depth and in 20-cm increments below that to 190 cm.

Four soil samples were taken at each depth with a Madera sampler. For the 10-cm depth the sampler was pushed vertically into the soil until the sampling volume was centered at 10 cm, the sampler was twisted to shear the soil at the bottom and then pulled out. For depths below 10 cm the soil was excavated on one side of the access tube and samples were taken by pushing or driving the sampler horizontally into the soil on either side of the access tube. Two samples were taken on opposite sides of the access tube just above and just below each reading depth in order to integrate the soil volume measured by the neutron probes. The Madera probe was chosen for soil sampling because its cutting edge is sharp and has a low cross-sectional area that reduces soil compaction, and because it is an open-ended sampler, which allows the operator to observe any soil compression or shattering that would compromise the sample. During sampling, if a sample was obviously compressed or shattered it was discarded and another taken adjacent. During data reduction the four samples were commonly averaged to give one water content per sampling depth for each access tube. However, the existence

of four samples per depth for each access tube allowed samples identified as outliers during regression analysis to be discarded, particularly if values of water content and bulk density for those samples were widely divergent from the mean of the other samples. Another advantage of the Madera probe is that it disturbs the soil outside the probe very little, thus allowing samples to be obtained within 1 or 2 cm of each other. Other volumetric samplers, such as ring samplers, tend to compress and disturb the soil greatly outside, and even in front of, the sampler as it is pushed into the soil.

A good range of water contents was achieved between the wet and dry sites (Fig. 12). Results of these techniques were very good (Table V). Root mean squared errors were less than 0.012 m^3 m^{-3} for all calibration equations, and often were on the order of 0.005 m^3 m^{-3}. There was no difference in the precision of calibration equations obtained for the two brands of moisture gauge. Enough samples were obtained to allow individual calibration equations to be calculated for the 10-cm depth, the 30- to 90-cm depth range, and the 110- to 190-cm depth range. There were important differences in the slopes and intercepts of these equations.

Earlier, similar results were obtained using these calibration techniques on a Pullman clay loam (Table VI) and a Ulysses silt loam (Table VII) (Evett, 1991, unpublished data). In the earlier study only two access tubes were installed in each site. The Pullman soil is a Paleustoll in the US taxonomy and has a strong Bt clay horizon (illuvial clay), and a calcic horizon with up to 45% by mass of $CaCO_3$. Distinctly different calibration equations were found for these two horizons as well as for the 10-cm depth. In 1993, field calibrations using these methods were done on the Ulysses silt loam and the Amarillo fine sandy loam (Table VII). Standard errors of estimate were less than 0.01 m^3 m^{-3} for all horizons, and there were important differences between calibration slopes for different horizons of the Amarillo soil. For the Ulysses soil, which lacks strong illuvial clay and calcic horizons, there was no important difference between calibration equations for any depth range below the 10-cm depth. Note that the calibration equations for probes with serial numbers 5447 and 6190 on the Amarillo soil changed between 1993 and 1995. Both gauges underwent repairs in the intervening period, causing the calibrations to change. Although the locations of these calibrations were different, they were in the same field and it is not expected that the differences in the equations between the two dates result from soil differences between the two locations.

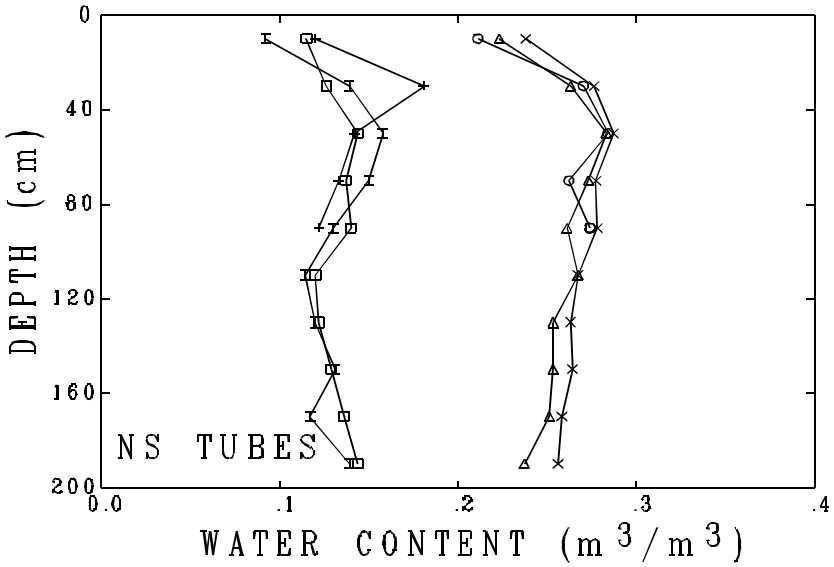

FIG. 12. Water content profiles at neutron scattering (NS) access tubes: dry site tubes: (□), (I), and (+); and wet site tubes: (X), (Δ), and (O).

TABLE V. REGRESSION EQUATIONS[a] FOR NEUTRON SCATTERING WATER CONTENT GAUGES IN AMARILLO FINE SANDY LOAM, BIG SPRINGS, TEXAS, USA [37].

Serial no.[b]	Model	Regression equation	r^2	RMSE[c] $m^3\ m^{-3}$	N
		A horizon (10-cm depth)			
5447	503DR	$\theta_v = 0.014 + 0.2172(CR)$	0.997	0.004	6
6190	503DR	$\theta_v = 0.001 + 0.2196(CR)$	0.999	0.002	6
0698	503DR	$\theta_v = 0.021 + 0.2105(CR)$	0.996	0.005	6
386	3331	$\theta_v = 0.054 + 0.5270(CR)$	0.992	0.006	6
385	3331	$\theta_v = 0.028 + 0.5388(CR)$	0.997	0.004	6
326	4301	$\theta_v = 0.001 + 0.4943(CR)$	0.999	0.002	6
		B horizon above calcic B (30- to 90-cm			
5447	503DR	$\theta_v = -0.066 + 0.2421(CR)$	0.988	0.008	24
6190	503DR	$\theta_v = -0.070 + 0.2464(CR)$	0.982	0.009	24
0698	503DR	$\theta_v = -0.070 + 0.2273(CR)$	0.989	0.007	24
386	3331	$\theta_v = -0.003 + 0.5206(CR)$	0.985	0.009	24
385	3331	$\theta_v = -0.016 + 0.5406(CR)$	0.985	0.009	24
326	4301	$\theta_v = -0.010 + 0.4646(CR)$	0.970	0.012	24
		Calcic B horizon (110- to 190-cm depth)			
5447	503DR	$\theta_v = -0.057 + 0.2299(CR)$	0.992	0.006	20
6190	503DR	$\theta_v = -0.062 + 0.2352(CR)$	0.992	0.006	20
0698	503DR	$\theta_v = -0.053 + 0.2086(CR)$	0.992	0.006	20
386	3331	$\theta_v = 0.001 + 0.5049(CR)$	0.993	0.006	20
385	3331	$\theta_v = -0.014 + 0.5276(CR)$	0.993	0.006	20
326	4301	$\theta_v = -0.017 + 0.4741(CR)$	0.992	0.006	20
		Complete B horizon (30- to 190-cm depth)			
5447	503DR	$\theta_v = -0.063 + 0.2371(CR)$	0.988	0.007	44
6190	503DR	$\theta_v = -0.067 + 0.2419(CR)$	0.984	0.008	44
0698	503DR	$\theta_v = -0.062 + 0.2189(CR)$	0.987	0.008	44
386	3331	$\theta_v = -0.001 + 0.5142(CR)$	0.988	0.007	44
385	3331	$\theta_v = -0.016 + 0.5360(CR)$	0.988	0.008	44
326	4301	$\theta_v = -0.013 + 0.4696(CR)$	0.979	0.010	44

[a] θ_v is water content ($m^3\ m^{-3}$), CR is the count ratio, which is the neutron count in the access tube divided by the standard count, and N is the number of samples in the regression analysis.

[b] Three-digit numbers refer to Troxler Electronic Laboratories gauges; four-digit numbers refer to Campbell Pacific Nuclear gauges.

[c] RMSE is root mean squared error.

TABLE VI. CALIBRATION EQUATIONS[a] FOR FOUR CPN NEUTRON MOISTURE GAUGES IN THE PULLMAN CLAY LOAM, BUSHLAND, TEXAS, USA, ILLUSTRATING EQUATIONS ESTABLISHED FOR DIFFERENT SOIL LAYERS (EVETT, 5-12 JUNE 1991, UNPUBLISHED DATA).

Ser. No. H35066190

Depth [cm]	Equation	N	r^2
10	θ_v = 0.0271 + 0.2442(CR)	7	0.91
30 - 210	θ_v = -0.0665 + 0.2641(CR)	39	0.96
30 - 110	θ_v = -0.1062 + 0.2908(CR)	19	0.96
130 - 210	θ_v = -0.0580 + 0.2599(CR)	20	0.97
30 - 130	θ_v = -0.0895 + 0.2798(CR)	23	0.95
150 - 210	θ_v = -0.0578 + 0.2593(CR)	16	0.97

Ser. No. H34055446

Depth [cm]	Equation	N	r^2
10	θ_v = -0.0036 + 0.2547(CR)	4	0.92
30 - 210	θ_v = -0.0618 + 0.2414(CR)	39	0.96
30 - 110	θ_v = -0.1009 + 0.2658(CR)	19	0.96
130 - 210	θ_v = -0.0532 + 0.2375(CR)	20	0.97
30 - 130	θ_v = -0.0862 + 0.2569(CR)	23	0.96
150 - 210	θ_v = -0.0528 + 0.2370(CR)	16	0.97

Ser. No. H34055447

Depth [cm]	Equation	N	r^2
10	θ_v = 0.0037 + 0.2583(CR)	4	0.90
30 - 210	θ_v = -0.0599 + 0.2484(CR)	39	0.96
30 - 110	θ_v = -0.0973 + 0.2724(CR)	19	0.96
130 - 210	θ_v = -0.0521 + 0.2450(CR)	20	0.97
30 - 130	θ_v = -0.0830 + 0.2633(CR)	23	0.96
150 - 210	θ_v = -0.0522 + 0.2451(CR)	16	0.97

Ser. No. H36046503

Depth [cm]	Equation	N	r^2
10	θ_v = 0.0013 + 0.2582(CR)	4	0.87
30 - 210	θ_v = -0.0624 + 0.2526(CR)	39	0.96
30 - 110	θ_v = -0.1025 + 0.2787(CR)	19	0.96
130 - 210	θ_v = -0.0534 + 0.2480(CR)	20	0.97
30 - 130	θ_v = -0.0861 + 0.2684(CR)	23	0.95
150 - 210	θ_v = -0.0528 + 0.2470(CR)	16	0.96

[a]The symbol θ_v is the water content ($m^3\ m^{-3}$), CR is the count ratio, which is the neutron count in the access tube divided by the standard count, and N is the number of samples in the regression analysis.

TABLE VII. CALIBRATION EQUATIONS[a] FOR AMARILLO AND ULYSSES SOILS FOR TWO CPN NEUTRON MOISTURE GAUGES (EVETT, 1993, UNPUBLISHED DATA).

AMARILLO fine sandy loam

Ser. No. 5447

Depth [cm]	Equation	N	SEE	r^2
10	θ_v = -0.0214 + 0.2505(CR)	6	0.0047	0.94
30 - 190	θ_v = -0.1048 + 0.2546(CR)	53	0.0063	0.95
30 - 90	θ_v = -0.0878 + 0.2435(CR)	24	0.0061	0.96
110 - 190	θ_v = -0.1328 + 0.2739(CR)	29	0.0055	0.96
30 - 110	θ_v = -0.0945 + 0.2482(CR)	30	0.0063	0.96
130 - 190	θ_v = -0.1291 + 0.2708(CR)	23	0.0054	0.96

Ser. No. 6190

Depth [cm]	Equation	N	SEE	r^2
10	θ_v = -0.0666 + 0.2984(CR)	6	0.0036	0.97
30 - 190	θ_v = -0.1139 + 0.2732(CR)	53	0.0066	0.95
30 - 90	θ_v = -0.0988 + 0.2636(CR)	24	0.0067	0.96
110 - 190	θ_v = -0.1415 + 0.2926(CR)	29	0.0052	0.97
30 - 110	θ_v = -0.1046 + 0.2676(CR)	30	0.0067	0.95
130 - 190	θ_v = -0.1391 + 0.2904(CR)	23	0.0052	0.97

ULYSSES silt loam

Ser. No. 5447

Depth [cm]	Equation	N	SEE	r^2
30 - 190	θ_v = -0.0321 + 0.2444(CR)	54	0.0076	0.98
30 - 90	θ_v = -0.0363 + 0.2469(CR)	24	0.0060	0.94
110 - 190	θ_v = -0.0331 + 0.2457(CR)	30	0.0088	0.98
30 - 110	θ_v = -0.0310 + 0.2424(CR)	30	0.0074	0.92
130 - 190	θ_v = -0.0368 + 0.2502(CR)	24	0.0073	0.99

Ser. No. 6190

Depth [cm]	Equation	N	SEE	r^2
30 - 190	θ_v = -0.0352 + 0.2579(CR)	54	0.0089	0.98
30 - 90	θ_v = -0.0436 + 0.2633(CR)	24	0.0077	0.90
110 - 190	θ_v = -0.0366 + 0.2598(CR)	30	0.0099	0.98
30 - 110	θ_v = -0.0383 + 0.2587(CR)	30	0.0085	0.90
130 - 190	θ_v = -0.0405 + 0.2648(CR)	24	0.0088	0.99

[a] θ_v is water content ($m^3\ m^{-3}$), CR is count ratio, SEE is standard error of estimate, N is the number of samples in the regression analysis.

2.2 **Temperature effect on standard counts**

Figure 13 shows data measured in 1985 using a Campbell Pacific Nuclear 503DR gauge during a field calibration exercise at Marana, Arizona. The calibration required the manual installation of access tubes and extraction of soil samples at several depths as the hole was augered. This was quite time consuming and installation of a particular access tube could finish at any time of the day. Just before taking count readings at the various depths in the access tube, a standard count in the shield was taken and the mean count, χ ratio and time were recorded. The gauge was in the field during the entire time and was equilibrated to air temperature as much as possible. A weather station in the field recorded air temperature every 15 minutes. The nearest 15 minute average air temperature and standard counts for which χ ratios were above 0.9 and below 1.1 were used to build the data set that is shown in the graph.

Linear regression (Fig. 13) showed that the ambient temperature explained 79% of the variation in standard count. The correlation was negative, with lower standard counts for higher temperatures. For a temperature change of 30 °C, one could expect a change in standard count of 177. The calibration equation for this probe had a slope of 3.59×10^{-5}. Multiplying the slope by the change in standard count gives a change in measured water content of 0.006 m^3 m^{-3}. This is close enough to a 1% change in water content to cause some concern.

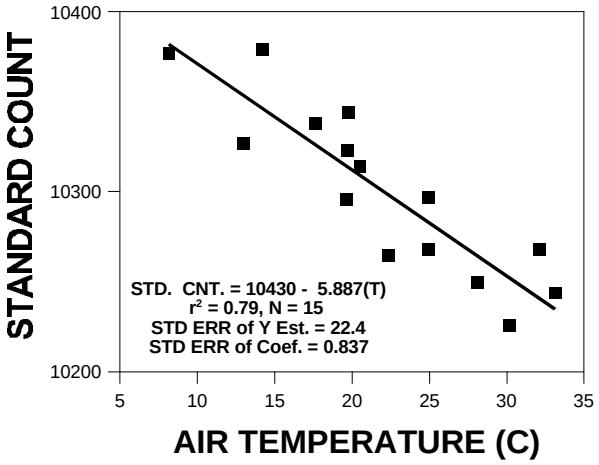

FIG. 13. Standard counts from a neutron moisture gauge (model 503DR, Campbell Pacific Nuclear International, Martinez, CA) and corresponding ambient air temperatures at Marana, Arizona, USA, 1985.

There are some reasons to expect that the primary source of temperature dependency is the detector tube, which contains boron trifluoride gas. Gas pressure is quite responsive to temperature changes and the detection process may be influenced by gas pressure. The counting circuitry may also be involved, particularly the high voltage and detector circuits, which are somewhat analog in nature. The rest of the circuitry in the probe would be insensitive to temperature because it is basically digital. Certainly the electronics in the gauge readout assembly, where the microcontroller is housed, are entirely digital so the problem almost certainly resides in the probe.

In the semiarid environment at Bushland, Texas, we may see a 17 °C air temperature swing during the working day. There is some potential for the probe to be subjected to even wider temperature swings because it is used in the access tube, as well as in the shield for standard counts. We don't have any idea what temperature the probe is at while it is in the access tube but we can be sure that it is changing. While traveling from one access tube to another the probe is locked in the shield and may equilibrate with ambient temperature. Once the probe is lowered to the bottom of the access tube it enters a much cooler or warmer environment depending on air temperature. The probe enters another temperature regime each time it is moved to a new depth stop for a reading. Because

we don't have a measure of probe or detector tube temperature we can't really correct for temperature swings. We can measure the effect from standard counts in the field or using an environmental housing set to different temperatures for each standard count. But, that information is useless to us unless we can measure the probe temperature during each reading in the access tube and during each routine standard count in the field.

2.3 **Suggestions for neutron probe calibration and use in a scientific setting**

1) Make sure there is a wide range in the water content data by finding or creating (eg., by growing a crop of sunflowers) a dry site, and then creating a wet site adjacent to it by berming an area and flooding it until the profile is wetted to the depth desired. Let drain to field capacity before sampling to avoid changes in water content due to drainage during sampling. The degree of spread in the water contents has a direct effect on the calibration equation r^2 value and thus the proportion of the variability in water content that is explained, through the calibration equation, by variations in count ratio. This is illustrated in Fig. 14. In Fig. 14a the original data for a wet and dry site calibration are shown along with the calibration equation, which had r^2 of 0.967 and SSE of 0.014 $m^3 m^{-3}$. In Figs. 14b and 14c the wet end data points have been moved closer to the dry end points. The relative positions of the points have not been changed and they have all been moved an equal distance along a line whose slope is equal to the regression slope for the unaltered data. Thus, the degree of noise in the data due to noise in counts or in volumetric water contents has not been altered. This fact is reflected in the standard error of estimate, which remained the same at 0.014 $m^3 m^{-3}$ for regressions on the altered data sets. But, the intercept became increasingly more negative and the slope more positive as the range of water contents decreased. For Fig. 14b the differences in slope and intercept were not large, but for Fig. 14c the slope increased by 0.039. This represents an error of about 0.04 $m^3 m^{-3}$ over a range of 1 in count ratio, which is equivalent to a water content range of about 0.26 $m^3 m^{-3}$ for the original data, or about a 16% error rate. The apparent invariant width of the 95% confidence intervals is misleading. Although the confidence intervals around the data points do not change, the confidence intervals outside the range of the data points (not plotted) increase dramatically, illustrating that another advantage of a wide range of water contents is greater confidence over the range of water contents likely to be encountered in the field.

2) Ensure adequate numbers of samples by installing at least three access tubes in both the wet and the dry sites, and by taking four samples around each tube at each depth that is read with the neutron probe. This typically gives enough samples that calibration equations can be broken out by soil layers or horizons (see Tables V-VII above), and the slopes can be shown with some confidence to be equivalent or not between layers. The 10 cm depth always requires a separate calibration equation due to loss of neutrons to the atmosphere; and enough samples should be taken around the access tubes to ensure a good calibration for this depth. With the Madera probe, six vertical samples can usually be obtained around each access tube for the 10 cm depth.

3) Ensure that samples are good ones. We do this by trenching alongside the access tubes and sampling horizontally around the tube with a Madera probe. This probe has a small cross sectional cutting area and is machined inside to a larger diameter past the cutting edge (Fig. 15). Thus, it compresses samples very little. Also, after driving in the probe, one can see easily if the sample is compressed, by comparing the soil surface inside and outside the probe body. Likewise, one can see if the sample is shattered, which would result in bulk density being too low for that sample. Bad samples can be discarded on the spot and replacement ones taken. Because this probe gives a 60 cm^3 sample volume, the volumetric water content can be determined directly and the heterogeneity of bulk density and water content assessed at each depth. With four samples per depth per tube, outliers can be discarded later if prudent and there will still be enough samples to give a good mean water content at each depth and tube. Our experience with ring samplers is that the extra width of the cutting edge, required to accommodate the ring inside the sampler, increases the cross sectional area of the cutting edge and thus increases compression of soil ahead of the sampler as it is driven into the soil. Trench walls are stair stepped or shored up to prevent collapse and injury to workers.

Note that the Madera probe was developed for sampling down the auger hole as access tubes were installed. Having used the probe extensively in this way I have concluded that the down-hole method is less desirable for two reasons. First, only one sample per depth is obtained. Second, despite the best care, samples may be compressed and there is no way to directly assess this with a down-hole sample.

Madera probes and accessories may be purchased from

Precision Machine Company, Inc.
2933 North 36th Street
Lincoln, NE 68504-2498 USA

Tel: 402.467.5528 FAX: 402.467.5530

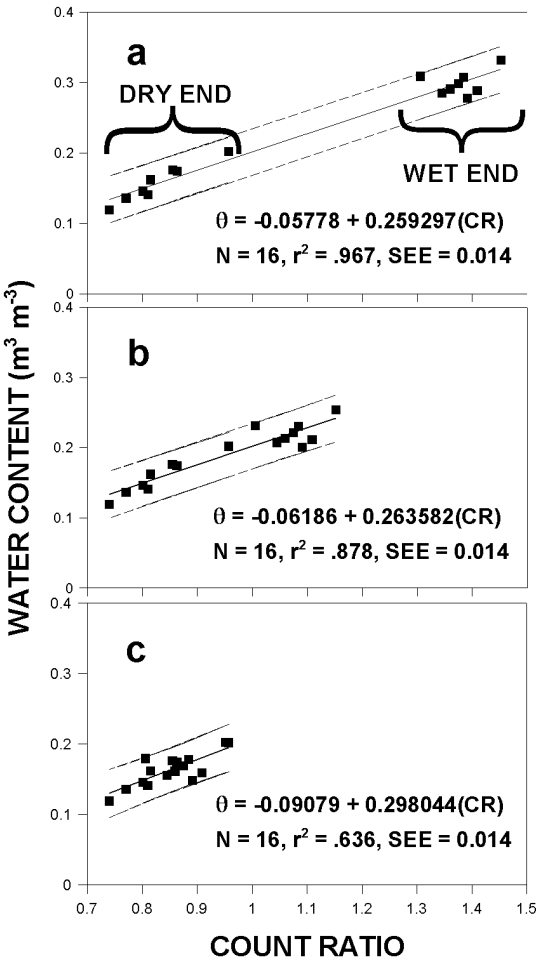

FIG. 14. An unaltered set of data from a wet site-dry site neutron probe calibration (a), and calibrations for the same data but with the wet end points moved closer (b) and still closer (c) to the dry end by sliding them along the regression slope. In each plot, the middle line is the regression line and the upper and lower lines are the 95% confidence intervals.

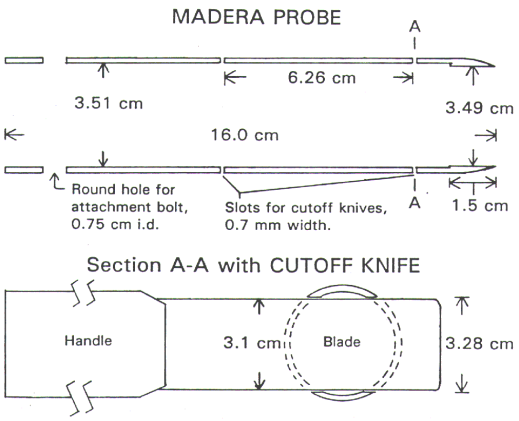

FIG. 15. Madera probe schematic.

They have probes for different soil types. Basically these offer thicker or thinner walls depending on soil resistance. At Bushland, we use the "clay" probes. We have not used the driver from PMCI. We just use a block of wood against the top of the probe and a 2 kg hammer to drive with. This probe works well because of the small cross sectional area normal to the axis of insertion, and the reamed body behind the cutting bit (Fig. 15), which relieves the core from frictional forces as it moves through the body of the probe. The bayonet mount ears on the top of the probe provide an ideal place to insert a rod to use to twist the probe before pulling it out of the soil. The twisting action shears the soil at the front end of the probe. We have found that lubricating the probe with silicone spray reduces compaction in some soils. Most of the lubricant is pushed off the probe by the first soil that passes through it so that negligible lubricant finds its way into the sample.

These probes have two slots for cutting the sample to produce the 60 cm^3 volumetric sample. Spatulas as sold by VWR, Cole-Parmer, PGC Scientifics, etc. will insert easily into these slots. One can do the same thing with spatulas sold in hardware stores, though most of these are too wide and must be ground to the right width on a bench grinder.

4) Ensure that the probe is at the correct depth for each reading. We take readings at 10-cm depth and in 20-cm increments below that. We have built stands (Fig. 16) that slide over the access tubes and keep the gauges a constant height above the soil surface (in our case 82 cm from gauge base to soil surface). We then set cable stops to give the desired depths of measurement. With this system we always get reading depths referenced to the soil surface, not to the top of the access tube. In normal field use, the user can march through the field quite readily with gauge in one hand and stand in the other. Other advantages of the stands are that the user can operate the gauge while standing, avoiding the back strain incurred when the gauge is set directly on top of the access tube, and that any interference of the gauge shield with the 10-cm depth reading is eliminated. Because cable stops may slide on the cable or the insulation may move up or down the cable, it is advisable to check the positions of cable stops periodically during the measurement season.

5) Ensure that standard counts are not influenced by soil water content. This is another advantage of the stands. We set up the stand on a base plate to take standard counts in the field away from vegetation (Fig. 17). Previous to this, we saw that standard counts varied depending on whether the soil was very wet after a heavy rain or dry (this with the gauge case set on the soil surface and the gauge set on the case for the standard count).

There are many other methods of neutron probe calibration. One that often gives good results involves sampling down multiple holes close to the access tube using the Madera probe to obtain volumetric soil samples at depths corresponding to neutron counting depths. An advantage of this method is that no trench is needed. Disadvantages included the lack of a visual check on sample

compression or shattering before the sample is removed, problems with obtaining a complete sample in sandier soils, and the care needed to center samples at the correct depths.

FIG. 16. A CPN model 503DR neutron probe mounted on a stand, which has been placed over an access tube. The feet of the stand are designed to fit between plants in a row, yet provide enough surface area to not sink into the soil. The protrusion of the access tube above the soil surface prevents the stand from falling over.

FIG. 17. On the left are the stand and base plate to support a neutron moisture gauge 82 cm above the soil for standard counts. On the right the stand is placed on the base plate and the neutron moisture gauge is in position for a shield count.

3. USE OF TDR AND NEUTRON SCATTERING FOR SOIL WATER BALANCE STUDIES

Weighing lysimeters have been used for many years for precise (e.g., 0.05 mm) measurement of evaporation (E) and evapotranspiration (ET) from bare and cropped soils [38]. However, lysimeter installations suffer from some serious drawbacks including disturbance of the soil profile, interruption of deep percolation and horizontal flow components and uneven management of lysimeter compared to field soil [39]. Other drawbacks include heat flux distortions caused by highly conductive steel walls [40, 41] and high cost, e.g., US$ 65,000 [42] and US$ 80,000 [43].

Alternatives to lysimetry for the measurement of E and ET (both mm) include mass balance techniques that involve measuring the components of the water balance equation for a soil profile of given depth:

$$\Delta S = P - (E \text{ or } ET) - D - R \quad (15)$$

where ΔS is the change in soil profile water storage, P is precipitation (including irrigation), R is runoff and D is deep percolation, i.e., water moving across the bottom boundary of the soil profile (all in mm). Solving for E or ET gives:

$$E \text{ or } ET = -\Delta S + P - D - R \quad (16)$$

Measurement intervals commonly range between hours and weeks and are usually no smaller than the required period of ET measurement. Measurement of each variable in the right-hand side of Eq. 16 presents its own unique problems, and it should be stated that lysimetry has three sources of measurement error as well (lysimeter mass (ΔS), precipitation (P), and runoff (R)). However, the water balance technique is applicable in many situations for which lysimetry is inappropriate or impossible and is, in addition, much less expensive. The focus of this section will be the measurement of changes in water storage, ΔS, using combined TDR and NS, compared with lysimeter measurements.

Soil profile water content measurement techniques range from destructive sampling using augers or coring tubes to non-destructive techniques such as gamma ray attenuation, neutron scattering and capacitance measurements in access tubes, and various sensors including resistance blocks, heat flux based sensors, and time domain reflectometry (TDR) probes that are buried at specific depths. Destructive techniques are commonly avoided due to the requirement to repeatedly measure the same locations and the time involved in handling the samples. Of the non-destructive techniques, neutron scattering (NS) was proposed by Van Bavel and Stirk in 1967 [44] for ET studies and has often been used since [45, 46]. Due to the small changes in water content associated with single day ET and the limited precision of NS, especially near the surface, the water balance method has usually been restricted to measurement of ET over several day periods [47]. Wright [46] compared ET measured by a weighing lysimeter to that measured by soil water balance using NS and concluded that large errors in the water balance method occurred if the depth of the profile measured by NS did not exceed the depth of wetting due to irrigation. The errors were then due to excessive water flux through the bottom of the profile.

Time domain reflectometry has more recently become available and lends itself to automated monitoring of soil water content [6, 7, 8, 9, 10]. One disadvantage of TDR is the difficulty of installing probes at depth. However, since the short term rapid changes in soil water content due to infiltration events and evaporation may be confined to the near surface layers, TDR may be used for these measurements while NS is used at greater depth. The spatial sensitivity of TDR may be confined to a region as small as 2 cm above and below the plane of horizontally installed probes [48, 49] so a great deal of information about the vertical variability of soil water content may be gathered relatively easily in the near surface soil, where such variation is most likely to occur and where the NS technique is most difficult to calibrate and properly apply. Evett et al. [9] investigated the joint use of TDR and NS for estimating ET and compared it to weighing lysimeter measurements as follows.

3.1. **Methods**

The experimental site was at Bushland, TX during 1992 from day of year (DOY) 80 to 108 in the northeast lysimeter field on a Pullman silty clay loam (fine, mixed, thermic Torrertic Paleustoll). The 3 m square by 2.3 m deep weighing lysimeter was in the center of a square 4.7 ha field. Lysimeter measurements of ET were precise to 0.05 mm [50]. Winter wheat was planted the previous fall and leaf area index increased from 4.2 to 6.7 over the experimental period while crop height varied from 20 to 60 cm.

Prior to planting wheat, TDR probes were installed in 2 vertical TDR/Temperature arrays in the lysimeter for measurement of soil water content. For each array, probes were installed horizontally at 2, 4, 6, 10, 15, 20 and 30 cm depths with Cu-Co thermocouples at the same depths. Probe traces were automatically measured and recorded at 30 min intervals using an IBM PC/XT compatible computer equipped with an analog to digital conversion card, and running a precursor to the TACQ program. A Tektronix model 1502 cable tester provided the TDR trace output. These older, analog cable testers are available for less than half the cost of the digital models and were modified for electronic control of trace output. A 16-channel multiplexer with 50 ohm characteristic impedance was designed to switch the TDR signals among probes while introducing minimal signal distortion (model TR-200, Dynamax, Inc, Houston, TX) [51]. Signals were provided through the PC's parallel port for both switching and toggling the cable tester for trace output.

Trifilar (three-wire) TDR probes were used (model TR-100, Dynamax, Inc., Houston, TX). Each consisted of an epoxy resin and polymethylmethacrylate handle from which extended three parallel, type 316 stainless steel rods. The rods were spaced in a single plane at 3 cm center to center and were 3.18 mm (nominal 1/8 inch) in diameter and 20 cm long from the tip to the point of emergence from the handle. The probes were inserted into the soil from the side of a pit so that the rods were parallel to the soil surface and the 3 rods for each probe were all the same distance from the soil surface. The outer two rods were soldered to the outer conductor of a type RG/58U coaxial cable and the inner rod was soldered to the inner conductor. The solder joints, proximal ends of the rods and distal end of the cable were encapsulated together in the handle. The three wire configuration is semi-coaxial in nature and eliminates the need for an impedance matching transformer (balun) used with a two rod design [18]. In addition, the range of sensitivity above and below the plane of the rods is narrower for the 3 wire configuration than for the 2 wire configuration most commonly used in the past [49], allowing for better discrimination of soil water content with depth.

The TDR method depends on the change in apparent permittivity of the soil that occurs when soil water content changes. The permittivity of the mineral matter in soil varies between 3 and 5. Although air may make up a large part of the soil volume, its permittivity is unity. By contrast, the permittivity of water is about 80 (depending on temperature). As soil wets and dries, its apparent permittivity, ε_a, changes accordingly, though not in a linear fashion. We computed ε_a as:

$$\varepsilon_a = \mu^{-1}[c_o t_T/(2L)]^2 \tag{17}$$

where t_T is the two way travel time in s for the cable tester voltage pulse to travel from one impedance change to the other and back again (i.e., round trip from probe handle to end of rods) as measured with TACQ, L is the distance in m between the impedance changes, c_o is the speed of light, m/s, and the magnetic permeability, μ, was assumed to be unity. For four fine-textured mineral soils, Topp et al. [1] experimentally determined a polynomial function describing the relationship between ε_a and volumetric water content, θ:

$$\theta = (-530 + 292\varepsilon_a - 5.5\varepsilon_a^2 + 0.043\varepsilon_a^3)/10^4 \tag{18}$$

The Pullman clay loam is a similar soil and Topp's equation was used.

The TDR water contents and first derivatives with respect to time were smoothed and calculated using center weighted quadratic polynomial least squares estimation with weights computed

using an algorithm that allows calculation of off-center weights for smoothing end points [22]. A nine-point data smooth followed by a five-point derivative smooth was used for water content data from the 2 to 20-cm depths. And, a 25-point data smooth followed by a fifteen-point derivative smooth was used for data from the 30-cm depth which, although noisier than that for shallower depths, did not change rapidly. Change in storage in mm per unit time was calculated by multiplying the layer thickness (mm) by the first derivative.

Water content measurements by NS were taken at two sites on each lysimeter at depths from 10 to 190 cm at 20-cm increments using a Campbell Pacific Nuclear model 503DR neutron moisture gauge. Access tubes were 4.1-cm (1.62 inch) ID, 4.4-cm (1.75 inch) O.D. steel electromechanical tubing, 2.3 m long. Counts were taken for 32 s. Prior to and after measurements, standard counts were taken until at least three standard counts were obtained with χ ratios in the range $0.9 \leq \chi$ ratio ≤ 1.1. Standard counts taken after the measurements in the tubes showed that no appreciable drift occurred over the measurement time. All standard counts were taken with the neutron probe sitting on top of its case, which rested on bare, dry soil. The Pullman soil has three horizons that differ in ways that are important for neutron probe calibration. Calibration equations for these are given in Table V above.

3.2. **Results**

Although only separated by 40 cm horizontal distance, the two TDR arrays showed markedly different soil wetness (Fig. 18). This was due to array 1 being in the inter-row where soil surface wetness tended to be lower and wetness at depth higher than for array 2 which was in the wheat row.

Despite this difference, data from the two arrays reflected very well the dynamics of multiple infiltration and drying sequences. Mean water storage changes in the top 40 cm of the soil profile followed closely the whole profile storage as measured by the lysimeter, including response to infiltration, daily drying and nighttime plateaus (Fig. 19).

The daily storage change measured by TDR averaged 88% of that measured by lysimeter confirming that by far the largest part of daily change in storage was in the top 40 cm of soil (Fig. 20). Implications of this are threefold. First, TDR arrays may be used to measure precisely the largest part of daily storage change. Second, the NS method, no matter how well calibrated, is unlikely to ever give good daily storage change measurements because it is most imprecise near the surface where most storage change occurs. Third, combining TDR with daily NS measurements holds great potential for precisely defining the daily change in soil profile water storage.

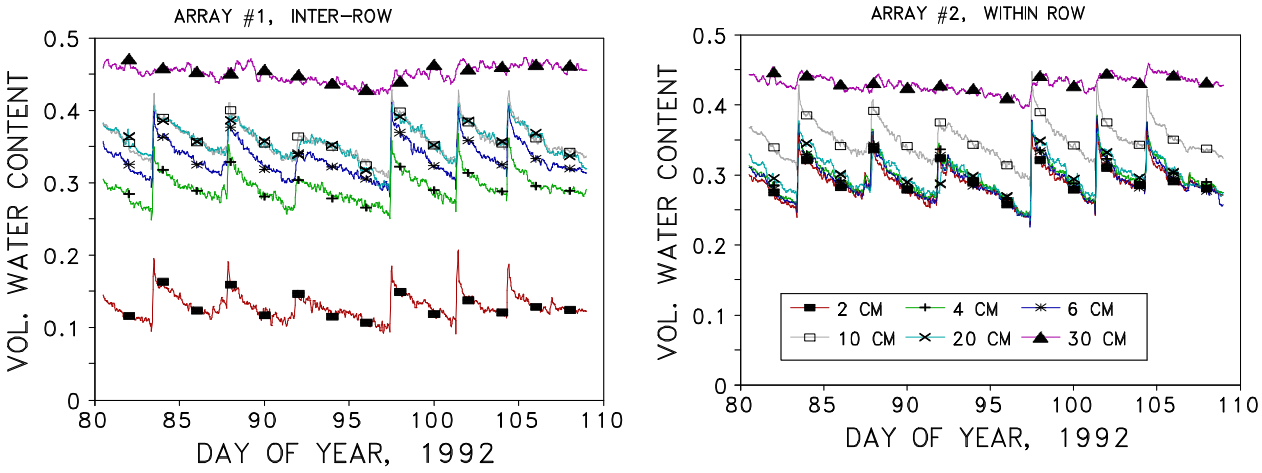

FIG. 18. Smoothed TDR water contents for two TDR arrays.

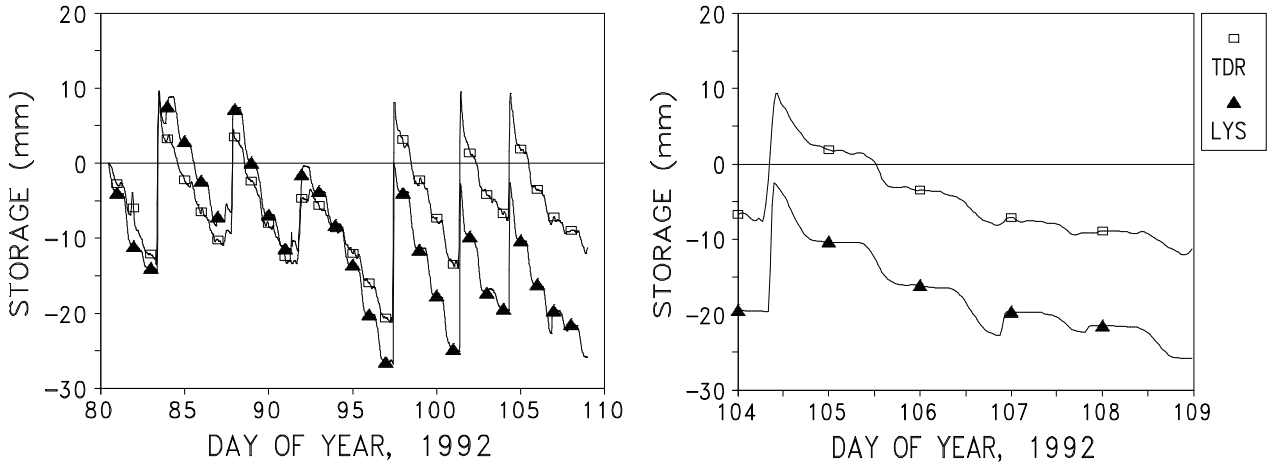

FIG. 19. Lysimeter (LYS) storage compared with mean storage from TDR for the entire period (left) and final five days (right).

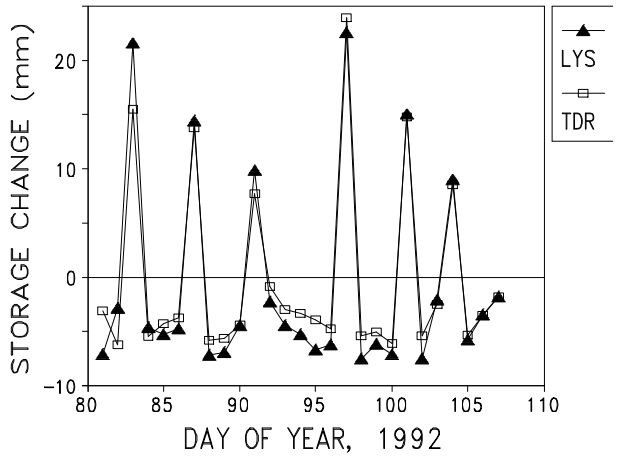

FIG. 20. Daily change in storage from lysimeter (LYS) and TDR arrays.

Deep percolation and runoff were zero for the lysimeter. Therefore, daily ET could be calculated from Eq. 16 by adding precipitation amount to storage change. There were large discrepancies between lysimeter measured ET and that calculated from change in storage based on TDR data alone (Fig. 21). The TDR method overestimated ET on precipitation (including irrigation) days in the first part of the period shown, due to drainage flux out of the bottom of the 0- to 40-cm layer. These precipitation events were followed by dry periods during which the TDR method underestimated ET due to upward soil water flux into the 0- to 40-cm layer.

Despite the underestimation, the TDR method followed the changes in daily ET well during the drying periods. Also, during the last 8 days of the period the TDR method matched closely the lysimeter measured ET even on days 101 (24 mm) and 104 (18 mm) when irrigation occurred. The good match for days 100 through 107 may be due to swelling of the B horizon after repeated precipitation and irrigation events. In this soil, once the cracks close the hydraulic conductivity decreases markedly, effectively sealing the bottom of the 0- to 30-cm soil layer. There is also some evidence that soil swelling may increase root axial resistance to water flow. This, combined with the tendency for the root system to remove water from the top soil layers first, may have caused most root water uptake to occur in the top 30 cm of soil. These results agree with those of Zegelin et al. [52], who found that TDR-measured changes in soil water storage agreed with lysimeter-measured values to better than 10% for a soil with a heavy clay subsoil.

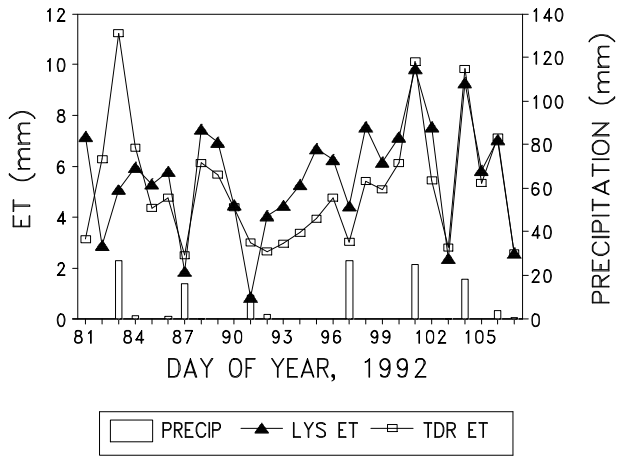

FIG. 21. Evapotranspiration calculated from lysimeter and TDR change in storage.

Lack of NS measurements precluded completion of the soil water balance on a daily basis. However, NS measurements on days 90 and 106 allowed the change in storage to be calculated for the intervening period. Lysimeter storage decreased by 9.31 mm over the 16-day period but NS measurements showed a 12.86-mm decrease or a 3.55-mm error. Combining the change in storage calculated for the 40- to 200-cm profile by NS with the TDR-based change in storage for the surface to 40-cm profile gave an 8.65-mm change in storage, for a smaller error of 0.67 mm.

Some insight into the problems involved in measuring near-surface soil water content with NS is given by Fig. 22, which shows NS measurements at 0.1 m and deeper, and TDR measurements at several depths in the top 0.2 m of soil. The vertical structure of water content near the surface is complex, with a layer at 0.1-m depth that is at 0.31 m^3 m^{-3} and which represents a wetting front from a recent rain. Just 5 cm below that layer the water content is only 0.22 m^3 m^{-3}. At 0.2-m depth the water content increases again due to the presence of an illuvial clay horizon. The NS measurement at 0.1-m depth appears to respond mostly to the water at 0.06 and 0.1-m depths, and not to the drier soil nearer the surface.

3.3. **Conclusions**

Vertical arrays of horizontally-installed TDR probes showed good potential for accurately measuring change in water storage in the top 40 cm of soil over periods of a day or less. Our TDR technology allowed us to show that, for our wheat crop, an average of 88% of the daily total soil profile change in storage occurred in the top 40 cm of soil. Since neutron scattering is most imprecise near the soil surface it thus becomes doubtful that neutron moisture gages alone could be used for daily ET estimates, no matter how well calibrated. However, the combination of neutron scattering measurements at depths below 40 cm with TDR measurements above 40 cm allowed the change in storage over a 16-day period to be calculated to within 0.7 mm of that measured by the weighing lysimeter. This error was one fifth of that realized when neutron scattering alone was used. Future research will combine daily neutron scattering measurements at depth with TDR measurements in the near surface soil of a lysimeter to find if accurate daily ET measurements can be made.

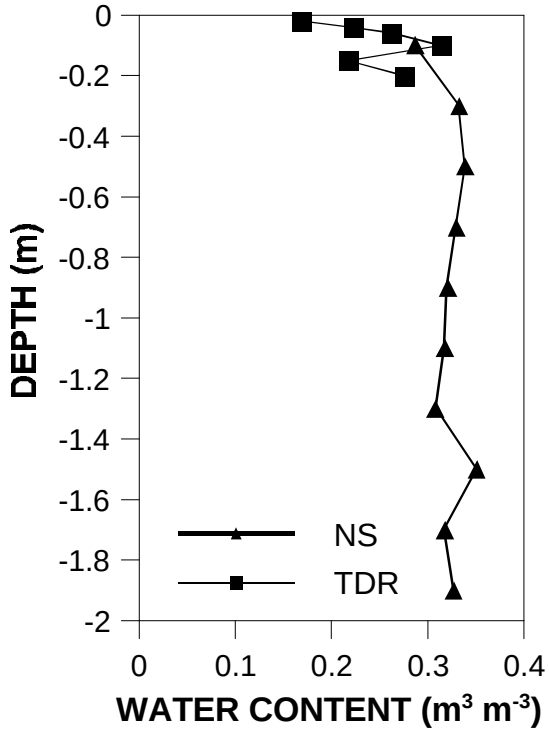

FIG. 22. TDR and neutron scattering (NS) measurements taken in a Pullman clay loam soil profile at Bushland, Texas, USA.

4. COMPARISON of NEUTRON and CAPACITANCE PROBES

A capacitance probe (CP) soil moisture gauge was described by Dean et al. [53]. The probe consists of an electrode pair separated by a plastic dielectric. The upper and lower electrodes and the plastic separator are in the shape of a cylinder that fits closely inside a plastic access tube. A resonant LC (L = inductance, C = capacitance) circuit in the probe includes the ensemble of the soil outside the access tube, the access tube itself, plus the air space between the probe and access tube, as one of the capacitive elements. Changes in the resonant frequency of the circuit depend on changes in the capacitance of the soil-access tube system. The difference between the resonant frequency of the probe in the access tube and a baseline resonant frequency (often measured with the probe in air) is called the D value and is the value reported by the gauges studied here.

Care is taken to center the capacitance probe in the access tube with minimal space between probe and tube. Access tube installation is also done so as to eliminate air gaps between the tube and soil and minimize soil disturbance. When these conditions are met, changes in the capacitance of the soil-access tube system are those induced by changes in soil water content, temperature, bulk density and macroporosity. The capacitance change caused by water content change is due to the high permittivity, ε_w (dimensionless), of water that is about 80 and is much higher than that of soil minerals (3 to 5) or air (1).

The capacitance of the soil-access tube system, C (F), is [53]:

$$C = g\varepsilon_a \tag{19}$$

where ε_a is the system apparent permittivity and g has units of farads and a value dependant on the geometry of the system. The resonant frequency, F (Hz), is [53]:

$$F = [2\pi(L)^{0.5}]^{-1} (C^{-1} + C_b^{-1} + C_c^{-1})^{0.5} \quad (20)$$

where C_b and C_c are the electrode capacitances (F) including the capacitances of internal circuit elements to which the electrodes are connected, C is the capacitance of the soil-access tube system defined in Eq. 17, and L is the inductance (henries) of the coil in the LC circuit. As soil water content increases, C also increases and *F* decreases. The temperature dependency is induced by the temperature dependence of water's permittivity (assuming that the probe electronics are practically temperature insensitive).

An idea of what the geometry parameter, *g*, refers to can be obtained from the classical equation for capacitance of a simple two electrode plate capacitor:

$$C = \varepsilon_o K_a a/d \quad (21)$$

where ε_o is the permittivity of free space (8.9×10^{-12} F/m), a is the overlapping area (m^2) of the plates and d is the thickness (m) of the dielectric separating the plates [54, Eq. 2-29]. This equation is valid only if the plates are parallel and the dielectric separating the plates is uniform. For this simple capacitor the value of *g* in Eq. 19 is $\varepsilon_o a/d$.

For the capacitance probe, the soil-access tube system that forms the dielectric between the two probe electrodes is complex, and no relationship has been established for computing *g* and thus C for this geometry. The plates take the form of two surfaces on a cylinder separated by an insulator, and the access tube and soil are outside of and not between the plates. Thus, the electric field permeating the soil forms a more or less elliptical torus around the probe with lines of force originating in one plate and ending in the other. This was called a *fringing field* by Thomas [55]. Although Eq. 21 does not apply to this configuration, any equation that did apply would have to include terms that describe the plate (electrode) surface area and the interaction of the electric field and the soil volume that it permeates. The latter is described by d in Eq. 21 since the simple geometry of a plate capacitor confines almost all the electromagnetic flux to the volume of dielectric between the plates. For the CP probe electrodes, the surface area of the electrodes is well known but the degree to which the torus of electric force lines permeates the soil is not. Thus, it seems that any term equivalent to d is particularly ill-defined in this soil-access tube system since the soil, with all its variability in bulk density and water content, becomes the dielectric in the capacitive system and the shape of the field may be influenced by soil heterogeneity including any gaps between the soil and tube wall induced by tube installation.

Bell et al. [56] described methods for access tube installation and calibration for this type of capacitance probe. Plastic tubes were installed, with a steel liner and cutting head operating through a guide plate to prevent lateral movement and the creation of air gaps between soil and tube. Installation proceeded in 4-cm increments using a screw auger placed inside the tube and augering no more than 4 cm ahead of the cutting head. All soil was placed in plastic bags and the procedure was assumed to provide a volumetric sample over a 4-cm depth. Calibration of the probe in four soils resulted in coefficients of determination (r^2) ranging from 0.55 to 0.74 for regressions of frequency shift, D (Hz), vs. volumetric water content for three soils, and r^2 of 0.86 and 0.92 for two horizons of the fourth soil. The latter calibration was based on four measurements. Comparison of predicted and measured soil water profiles indicated good correspondence, but the r^2 of some calibrations suggested that standard errors of estimate might be high.

A soil water content CP gauge (Troxler Electronic Laboratories, Inc., model SENTRY 200AP) was patterned after that of Dean et al. [53] and included some improvements while retaining the desired characteristics. Heathman [57] reported an r^2 of 0.62 for a field calibration of this gauge. Evett and Steiner [37] conducted a rigorous field calibration of four of the Troxler gauges in comparison with six neutron scattering (NS) gauges, using wet and dry sites as described above. Calibrations for the CP gauges exhibited low r^2 values, ranging from 0.04 to 0.71, and root mean squared error values of 0.036 to 0.058 $m^3\ m^{-3}$ (Table VIII). Example plots illustrate the much greater scatter of CP gauge data as compared with NS gauge data (Figs. 23-24).

In preliminary data analysis, Evett and Steiner [37] used stepwise linear regression of θ against frequency shift, D, D^2, soil bulk density, ρ (Mg m^{-3}), ρ^2, and $\rho^{0.5}$ to find the independent variable(s) that were a significant source of variability in the dependent variable. Other than the intercept, only the coefficient for D^2 was significant at the 0.50 level of probability. For the model, $\theta_v = B_0 + B_1D^2$, the coefficient for D^2 was so low ($B_1 = 4.6 \times 10^{-8}$) that the plot of θ_v vs. D was nearly linear and differed only slightly from a plot of the linear model. Because of this and the low significance of the $\theta_v = B_0 + B_1D^2$ relationship, this model was omitted from further consideration.

Some possible sources of variability in the CP gauge readings can be discounted. For instance, Dean et al. [53] showed that, for their design, total thermal (0 to 30 °C) and temporal (over 3 h) stability errors amounted to <0.005 m^3 m^{-3} error in water content. They also showed that air gaps between the tube and soil would introduce large errors, thus the exacting tube installation procedure. They did not measure the probe's sensitivity to ρ variations. But, in a companion paper, Bell et al. [56] noted that ρ appeared to affect the slope of calibration equations and concluded that more work was required in this area.

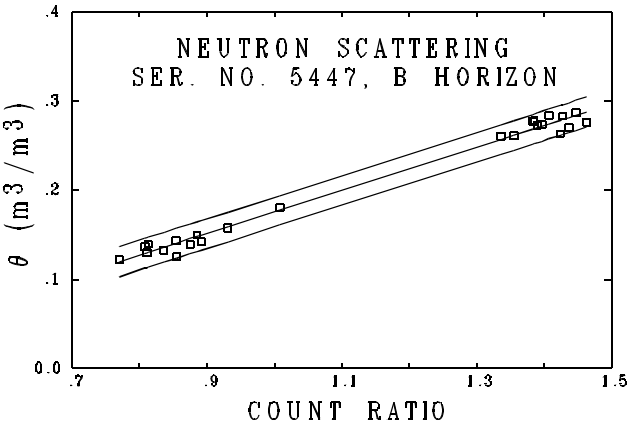

FIG. 23. Typical volumetric water content (q) vs. count ratio relationship in the B horizon (tubes 1-6). Middle line is the regression line, upper and lower lines are 95% confidence limits on the predictions

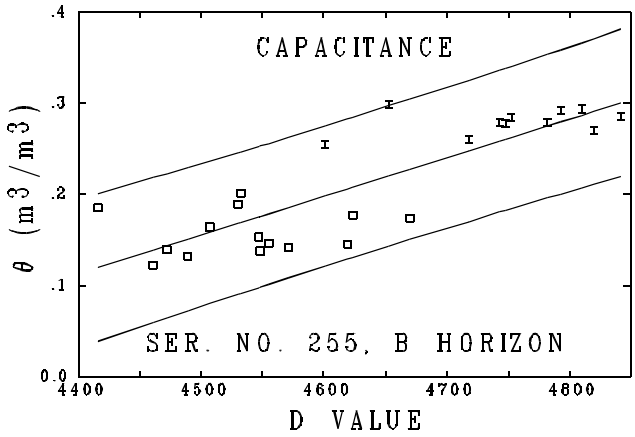

FIG. 24. Typical relationship between volumetric water content (q) and the absolute value of the measured frequency shift (D) from capacitance gauges (tubes 7-13), showing dry site data (□) and wet site data (I). Middle line is the regression line, upper and lower lines are 95% confidence limits on predictions.

TABLE VIII. REGRESSION EQUATIONS FOR THE CAPACITANCE TYPE WATER CONTENT GAUGES; WATER CONTENT (θ_v)VS. D VALUE, AND D VALUE VS. MEAN D VALUE.

Serial no.	Regression equation	r^2	RMSE[a] $m^3\ m^{-3}$	N
	A horizon (10-cm depth)			
255	$\theta_v = -0.140 + 0.000073(D)$	0.041	0.058	7
256	$\theta_v = -0.700 + 0.000215(D)$	0.211	0.052	7
257	$\theta_v = -0.273 + 0.000115(D)$	0.019	0.058	7
294	$\theta_v = -0.110 + 0.000067(D)$	0.010	0.058	7
	B horizon (41- to 102-cm depth)			
255	$\theta_v = -1.750 + 0.000423(D)$	0.698	0.036	25
256	$\theta_v = -1.460 + 0.000365(D)$	0.712	0.036	25
257	$\theta_v = -1.404 + 0.000380(D)$	0.681	0.037	25
294	$\theta_v = -1.583 + 0.000410(D)$	0.704	0.036	25
	D value vs. Mean D value (41- to 102-cm depth)			
255	D = 500 + 0.93(Mean D)	0.970	23	25
256	D = -271 + 1.09(Mean D)	0.974	25	25
257	D = -339 + 1.03(Mean D)	0.989	16	25
294	D = 110 + 0.96(Mean D)	0.960	27	25

[a]RMSE is root mean squared error.

The CP gauge is responsive mostly to a soil layer as thin as 8 cm [56] or 12 cm [58] vertically, and within 11 cm of the probe centerline [58]. Thus, small-scale variations in soil properties are more likely to influence the probe's readings than would be the case for the NS gauge. Our soil samples were generally taken within the 11-cm radius and 12-cm vertical range but there was considerable variation in individual water contents for a given depth and access tube. The electric field induced in the soil by the CP is influenced by boundaries between soil volumes having different permittivities [53]. Thus, ρ or θ_v variations on a small scale could set up boundaries that would influence the size and shape of the sampled volume. Boot and Watson [59] noted that sample heterogeneities can cause anomalous readings from capacitance probes applied to building materials, especially when the wavelength approaches the scale of heterogeneity. Wobschall [60] pointed out that heterogeneous soils can also cause poor results.

Another possible explanation for the poor results with the CP gauges is that the measurement volume is considerably smaller than reported by Bell et al. [56] and Troxler Electronic Laboratories [58]. If this were so then the soil sampling method that we used would be inappropriate. However, the 15.24-cm measurement interval provided by the stops on the CP gauge probe handle would be too large if the sampling volume were smaller than that stated by Troxler Electronic Laboratories [58]. If the sampling volume is indeed much smaller than reported, then the use of the CP gauge must be reevaluated because many more samples at much smaller vertical sampling intervals must be taken to provide accurate integration of the soil water content profile. In fact, if this hypothesis is true it may

be difficult to accurately portray the soil water content profile in many soils because the representative elemental volume may be larger than the gauge's sampling volume. Field calibration of this gauge would also be problematic in this case because an exacting relationship between probe position in the tube and position of soil sampling is implied.

Tomer and Anderson [61] obtained better results with the Troxler CP gauge in a comparison with an NS gauge in a deep aeolian sand (Zimmerman fine sand). Samples for calibration were obtained by taking 5 cm diameter vertical cores. Access tubes were then installed in the coring holes. Because the sand was not cohesive, bulk density values were not used from these samples, but bulk densities from a previous study were used to calculate volumetric water contents. The NS gauges calibration resulted in an r^2 value of 0.966 (N = 31). The CP gauge calibration gave an r^2 value of 0.888 (N = 73), and was similar to the manufacturer's calibration equation, a fact that is not surprising given that the manufacturer calibrates in sand. Soil water lost in a 1.5 m profile over 2 weeks averaged 1.2 cm less as measured by the CP gauge compared with the NS gauge, and the CP gauge routinely gave higher water content measurements. The CP gauge had much higher spatial resolution, a fact that rendered it susceptible to problems with access tube installation.

Mohamed et al. [62] compared the Humicap (Nardeux, Loches, France) capacitance probe to a neutron probe (Solo 25, Nardeux, Loches, France). The capacitance probes were buried in augered holes with direct contact between the electrodes and the soil. The capacitance probes were "highly sensitive to change in soil structure and texture," but provided better accuracy than the neutron probe, which was calibrated by a theoretical method. It is likely that the better results obtained for capacitance probes in this study were due to the lack of an air gap between the electrodes and the soil.

Paltineanu and Starr [63] calibrated a capacitance probe (EnvironSCAN, Sentek Pty Ltd., South Australia) in the laboratory using a silt loam soil with good results (r^2 = 0.992, N = 15, θ_v range = 0.07 - 0.37 $m^3\ m^{-3}$, RMSE = 0.009 $m^3\ m^{-3}$). Their calibration equation was

$$\theta_v = 0.490\ SF^{2.1674} \tag{22}$$

where SF is the dimensionless scaled frequency

$$SF = (F_a - F_s)(F_a - F_w)^{-1} \tag{23}$$

where F_a and F_w are readings in air and water, respectively, and F_s is the reading in the access tube (all in Hz). Boxes were packed very uniformly (CV for ρ_b = 0.5 to 2.9%, CV for θ_v = 0.0054 to 0.065%) with soil at four different water contents for the calibration. The extreme uniformity of packing brings into question how appropriate the calibration would be for a field soil, which is likely to be much less uniform in bulk density and water content on a small scale. Tests of radial sensitivity showed that 99% of the sensitivity was within a 10 cm radius outside of the access tube, and 92% of the sensitivity was within a 3 cm radius of soil outside the access tube (Fig. 25). This reveals that the probe will be quite sensitive to small scale variations of soil properties close to the access tube. Later, the same authors [64] installed these probes in the field for long term measurements of profile water content. Though they reported success, they did not test to determine if the laboratory calibration proved accurate in the field. The tests they did conduct were comparisons with crop water use estimated using an atmometer, and cannot be considered rigorous. Oddly, they did not report any water contents, only soil water storage and change in storage data. Paltineanu and Starr [63] considered it inappropriate to compare the capacitance method with neutron scattering due to differences in measurement method and sphere of influence. However, such differences might well be the point of a comparison, as was shown by Evett and Steiner [37].

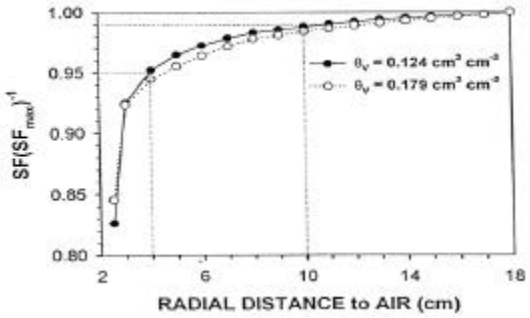

FIG. 25. Relative radial sensitivity of EnviroScan sensors as a function of radial thickness of soil around the access tube (from [63]).

At this writing (1998), many capacitance type soil moisture probes or gauges are being introduced in the marketplace. Some of these respond quite well to the dynamics of soil water content, including that due to plant water uptake. Demonstrations have shown that the dynamic behavior of plant water uptake can provide important information needed for irrigation scheduling. But, there is a lack of scientific literature supporting claims of accuracy of soil water content measurement with these devices, demonstrating that laboratory calibrations may be used successfully in the field, or demonstrating successful field calibrations. Capacitance probes that employ sensors in a plastic access tube are the closest analogue of the neutron probe deployed in an access tube. However, studies to date show that capacitance probes have a very narrow radial range of sensitivity outside of the access tube and thus suffer from disadvantages that include 1) sensitivity to soil disturbance during tube installation, and 2) sensitivity to small scale variations in soil bulk density (including macroporosity), water content, and texture, which are common to many soils. Other studies have shown that capacitance probes are still sensitive to soil salinity, temperature, and texture, though perhaps less so than in the past. Though it may be useful for some irrigation scheduling needs, the capacitance probe still cannot be considered a replacement for the neutron probe for soil water content measurements for which accuracy is important.

REFERENCES

[1] TOPP, G.C., DAVIS, J.L., AND ANNAN, A.P. Electromagnetic determination of soil water content: Measurements in coaxial transmission lines. Water Resour. Res. 16(3) (1980) 574-582.

[2] DALTON, F.N., HERKELRATH, W.N., RAWLINS, D.S., AND RHOADES, J.D. Time-domain reflectometry: simultaneous measurement of soil water content and electrical conductivity with a single probe. Science 224 (1984) 989-990.

[3] DALTON, F.N., AND VAN GENUCHTEN, M. TH. The time-domain reflectometry method for measuring soil water content and salinity. Geoderma 38 (1986) 237-250.

[4] DASBERG, S., AND DALTON, F.N. Time domain reflectometry field measurements of soil water content and electrical conductivity. Soil Sci. Soc. Am. J. 49 (1985) 293-297.

[5] TOPP, G.C., YANUKA, M., ZEBCHUK, W.D., AND ZEGELIN, S. Determination of electrical conductivity using time domain reflectometry: Soil and water experiments in coaxial lines. Water Resour. Res. 24 (1988) 945-952.

[6] BAKER, J.M., AND ALLMARAS, R.R. System for automating and multiplexing soil moisture measurement by time-domain reflectometry. Soil. Sci. Soc. Am. J. 54(1) (1990) 1-6.

[7] HEIMOVAARA, T.J., AND BOUTEN, W. A computer-controlled 36-channel time domain reflectometry system for monitoring soil water contents. Water Resour. Res. 26(10) (1990) 2311-2316.

[8] HERKELRATH, W.N., HAMBURG, S.P., AND MURPHY, F. Automatic, real-time monitoring of soil moisture in a remote field area with time domain reflectometry. Water Resour. Res. 27(5) (1991) 857-864.

[9] EVETT, S.R., HOWELL, T.A., STEINER, J.L., AND CRESAP, J.L. Evapotranspiration by soil water balance using TDR and neutron scattering. In Management of Irrigation and Drainage Systems, Irrigation and Drainage Div./ASCE, July 21-23, 1993, Park City, Utah. pp. 914-921 (1993).

[10] EVETT, S.R. TDR-Temperature arrays for analysis of field soil thermal properties. Pp. 320-327 In Proceedings of the Symposium on Time Domain Reflectometry in Environmental, Infrastructure and Mining Applications, Sept. 7-9, 1994. Northwestern University, Evanston, Illinois (1994).

[11] TOPP, G.C., DAVIS, J.L., AND ANNAN, A.P. Electromagnetic determination of soil water content using TDR: I. applications to wetting fronts and steep gradients. Soil Sci. Soc. Am. J. 46 (1982) 672-678.

[12] HEIMOVAARA, T.J. Design of triple-wire time domain reflectometry probes in practice and theory. Soil Sci. Soc. Am. J. 57 (1993) 1410-1417.

[13] EVETT, S.R. The TACQ program for automatic measurement of water content and bulk electrical conductivity using time domain reflectometry. Presented at the 1998 Annual International Meeting Sponsored by ASAE. ASAE Paper No. 983182. ASAE, 2950 Niles Road, St. Joseph, MI 49085-9659 USA (1998b).

[14] LEDIEU, J., DE RIDDER, P., DE CLERCK, P., AND DAUTREBANDE, S. A method of measuring soil moisture by time-domain reflectometry. J. Hydrol. 88 (1986) 319-328.

[15] WILLIAMS, T. The Circuit Designer's Companion. Butterworth-Heinemann, Ltd., Oxford, Pub. 302 pp. (1991).

[16] SAVITSKY, A., AND GOLAY, M.J.E. Smoothing and differentiation of data by simplified least squares. Anal. Chem. 36 (1964) 1627-1639.

[17] SPAANS, E.J.A., AND BAKER, J.M. Simple baluns in parallel probes for time domain reflectometry. Soil Sci. Soc. Am. J. 57 (1993) 668-673.

[18] ZEGELIN, S.J., WHITE, I., AND JENKINS, D.R. Improved field probes for soil water content and electrical conductivity measurement using time domain reflectometry. Water Resour. Res. 25(11) (1989) 2367-2376.

[19] HOOK, W.R., AND LIVINGSTON, N.J. Propagation velocity errors in time domain reflectometry measurements of soil water. Soil Sci. Soc. Am. J. 59 (1995) 92-96.

[20] WRAITH, J.M., COMFORT, S.D., WOODBURY, B.L., AND INSKEEP, W.P. A simplified waveform analysis approach for monitoring solute transport using time-domain reflectometry. Soil Sci. Soc. Am. J. 57 (1993) 637-642.

[21] HOOK, W.R., LIVINGSTON, N.J., SUN, Z.J., AND HOOK, P.B. Remote diode shorting improves measurement of soil water by time domain reflectometery. Soil Sci. Soc. Am. J. 56 (1992) 1384-1391.

[22] GORRY, P.A. General least-squares smoothing and differentiation by the convolution (Savitsky-Golay) method. Anal. Chem. 62 (1990) 570-573.

[23] WRAITH, J.M., AND OR, D. Temperature effects on time domain reflectometry measurement of soil bulk dielectric constant: experimental evidence and hypothesis development. Water Resour. Res. (in press)

[24] DALTON, F.N. Measurement of soil water content and electrical conductivity using time-domain reflectometry. In Proceedings of the International Conference on Measurement of Soil and Plant Water Status. July 6-10, 1987, Utah State University, Logan. Vol. 1, (1987) 95-98.

[25] DALTON, F.N. Development of time domain reflectometry for measuring soil-water content and bulk soil electrical conductivity. Pp. 143-167 In G.C. Topp, W.D. Reynolds, and R.E. Green (eds) Advances in Measurement of Soil Physical Properties: Bringing Theory into Practice. Soil Sci. Soc. Am., Madison, WI. (1992).

[26] NADLER, A., DASBERG, S., AND LAPID, I. Time domain reflectometry measurements of water content and electrical conductivity of layered soil columns. Soil Sci. Soc. Am. J. 55 (1991) 938-943.

[27] BAKER, J.M., SPAANS, E.J.A., AND REECE, C.F. Conductimetric measurement of CO_2 concentration: Theoretical basis and its verification. Agron. J. 88 (1996) 675-682.

[28] GARDNER, W., AND KIRKHAM, D. Determination of soil moisture by neutron scattering. Soil Sci. 73 (1952) 391-401.

[29] VAN BAVEL, C.H.M., UNDERWOOD, N., AND SWANSON, R.W. Soil moisture measurement by neutron moderation. Soil Sci. 82 (1956) 29-41.
[30] GARDNER, W.H. Water content. p. 493-544 *In* A. Klute (ed.) Methods of soil analysis, Part 1. 2nd ed. Agron. Monogr. 9. ASA and SSSA, Madison, WI. (1986).
[31] GREACEN, E.L. Soil water assessment by the neutron method. CSIRO, Melbourne, Australia. (1981).
[32] STONE, J.F., ALLEN, R.G., DICKEY, G.L., WRIGHT, J.L., NAKAYAMA, F.S., AND PHILLIPS, R.W. The ASCE neutron probe calibration study: Overview. Pp. 1095- 1102 *In* R.G. Allen and C.M.U. Neale (eds.) Management of Irrigation and Drainage Systems, Integrated Perspectives. Am. Soc. Civil Engr., New York, NY. Proceedings of the National Conference on Irrigation and Drainage Engineering, Park City, UT, July 21-23, 1993. (1993a).
[33] STONE, J.F., ALLEN, R.G., GRAY, H.R., DICKEY, G.L., AND NAKAYAMA, F.S. Performance factors of neutron moisture probes related to position of source on detector. Pp. 1128-1135 *In* R.G. Allen and C.M.U. Neale (eds.) Management of Irrigation and Drainage Systems, Integrated Perspectives. Am. Soc. Civil Engr., New York, NY. Proceedings of the National Conference on Irrigation and Drainage Engineering, Park City, UT, July 21-23, 1993. (1993b).
[34] DICKEY, G.L., ALLEN, R.G., BARCLAY, J.H., WRIGHT, J.L., STONE, J.F., AND DRAPER, B.W. Neutron gauge calibration comparison of methods. Pp. 1136- 1144 *In* R.G. Allen and C.M.U. Neale (eds.) Management of Irrigation and Drainage Systems, Integrated Perspectives. Am. Soc. Civil Engr., New York, NY. Proceedings of the National Conference on Irrigation and Drainage Engineering, Park City, UT, July 21-23, 1993. (1993a).
[35] ALLEN, R.G., DICKEY, G., WRIGHT, J.L. Effect of moisture and bulk density sampling on neutron moisture gauge calibration. Pp. 1145-1152 *In* Management of irrigation and drainage systems, integrated perspectives. Proceedings of the 1993 ASCE national conference on irrigation and drainage engineering, Park City, UT, July 21-23, 1993. (1993a).
[36] DICKEY, G.L., ALLEN, R.G., WRIGHT, J.L., MURRAY, N.R., STONE, J.F., AND HUNSAKER, D.J. Soil bulk density sampling for neutron gauge calibration. Pp. 1103-1111 *In* R.G. Allen and C.M.U. Neale (eds.) Management of Irrigation and Drainage Systems, Integrated Perspectives. Am. Soc. Civil Engr., New York, NY. Proceedings of the National Conference on Irrigation and Drainage Engineering, Park City, UT, July 21-23, 1993. (1993b).
[37] EVETT, S.R., AND STEINER, J.L. Precision of neutron scattering and capacitance type moisture gages based on field calibration. Soil Sci. Soc. Am. J. 59 (1995) 961-968.
[38] HOWELL, T.A., SCHNEIDER, A.D., AND JENSEN, M.E. History of lysimeter design and use for evapotranspiration measurements. Pp. 1-9 in Lysimeters for evapotranspiration and environmental measurements, Proceedings of the International Symposium on Lysimetry, July 23-25, 1991, Honolulu, Hawaii. ASCE, 345 E. 47th St., NY, NY 10017-2398. (1991).
[39] GREBET, R., AND CUENCA, R.H. History of lysimeter design and effects of environmental disturbances. Pp. 10-18 in Lysimeters for evapotranspiration and environmental measurements, Proceedings of the International Symposium on Lysimetry, July 23-25, 1991, Honolulu, Hawaii. ASCE, 345 E. 47th St., NY, NY 10017-2398. (1991).
[40] BLACK, T.A., THURTELL, G.W., AND TANNER, C.B. Hydraulic load cell lysimeter, construction, calibration and tests. Soil Sci. Soc. Am. Proc. 32 (1968) 623-629.
[41] DUGAS, W.A., AND BLAND, W.L. Springtime soil temperatures in lysimeters in Central Texas. Soil Sci. 152(2) (1991) 87-91.
[42] LOURENCE, F., AND MOORE, R. Prefabricated weighing lysimeter for remote research stations. Pp. 432-439 in Lysimeters for evapotranspiration and environmental measurements, Proceedings of the International Symposium on Lysimetry, July 23-25, 1991, Honolulu, Hawaii. ASCE, 345 E. 47th St., NY, NY 10017-2398. (1991).
[43] MAREK, T.H., SCHNEIDER, A.D., HOWELL, T.A., AND EBELING, L.L. Design and construction of large weighing monolithic lysimeters. Trans. ASAE 31 (1988) 477-484.
[44] VAN BAVEL, C.H.M., AND STIRK, G.B. Soil water measurement with and Am^{241}-Be neutron source and an application to evaporimetry. J. Hydrol. 5 (1967) 40-46.
[45] CUENCA, R.H. Model for evapotranspiration using neutron probe data. J. Irrig. and Drain. Engrg., ASCE, 114(4) (1988) 644-663.

[46] WRIGHT, J.L. Comparison of ET measured with neutron moisture meters and weighing lysimeters. Pp. 202-209 in Irrigation and drainage: proceedings of the National Conference. Durango, Colorado, July 11-13, 1990. ASCE, 345 E. 47th St., NY, NY 10017-2398. (1990).

[47] CARRIJO, O.A., AND CUENCA, R.H. Precision of evapotranspiration estimates using neutron probe. J. Irrig. and Drain. Engrg., ASCE, 118(6) (1992) 943-953.

[48] BAKER. J.M., AND LASCANO, R.J. The spatial sensitivity of time-domain reflectometry. Soil Sci. 147 (1989) 378-384.

[49] ALSANABANI, M.M. Soil water determination by time domain reflectometry: sampling domain and geometry. Ph.D. thesis. Department of Soil and Water Sciences, Univ. of Arizona, Tucson, AZ 85721. (1991).

[50] HOWELL, T.A., SCHNEIDER, A.D., DUSEK, D.A., AND MAREK, T.H. Calibration of Bushland weighing lysimeters and scale performance as affected by wind. ASAE Paper No. 87-2505. American Society of Agricultural Engineers, St. Joseph, Missouri. (1987)

[51] EVETT, S.R. Coaxial multiplexer for time domain reflectometry measurement of soil water content and bulk electrical conductivity. Trans. ASAE 42(2) (1998) 361-369.

[52] ZEGELIN, S.J., WHITE, I., AND RUSSELL, G.F. A critique of the time domain reflectometry technique for determining field soil-water content. Pp. 187-208 In G.C. Topp, W.D. Reynolds, and R.E. Green (eds) Advances in Measurement of Soil Physical Properties: Bringing Theory into Practice. Soil Sci. Soc. Am., Inc., Madison, WI. (1992).

[53] DEAN, T.J., BELL, J.P., AND BATY, A.J.B. Soil moisture measurement by an improved capacitance technique: Part I. Sensor design and performance. J. Hydrol. (Amsterdam) 93 (1987) 67-78.

[54] MALMSTADT, H.V., ENKE, C.G., CROUCH, S.R., AND HORLICK, G. Electronic measurements for scientists. W.A. Benjamin, Menlo Park, CA. (1974).

[55] THOMAS, A.M. *In situ* measurement of moisture in soil and similar substances by 'fringe' capacitance. J. Sci. Instrum. 43 (1966) 21-27.

[56] BELL, J.P., DEAN, T.J., AND HODNETT, M.G. Soil moisture measurement by an improved capacitance technique: Part II. Field techniques, evaluation and calibration. J. Hydrol. (Amsterdam) 93 (1987) 79-90.

[57] HEATHMAN, G.C. Soil moisture determination using a resonant frequency capacitance probe. Paper no. 931053. American Society of Agricultural Engineers, St. Joseph, MI. (1993).

[58] TROXLER ELECTRONIC LABORATORIES. Troxler technical brief: Comparing the Sentry 200-AP and the model 4300 moisture probes. Troxler Electronic Lab., Research Triangle Park, NC. (1993).

[59] BOOT, A.R., AND WATSON, A. Applications of centrimetric radio waves in nondestructive testing. p. 3-24 *In* ASTM-RILEM Symp. Appl. Adv. Nucl. Phys. Testing Materials. Texas A&M University, College Station. (1964).

[60] WOBSCHALL, D. A frequency shift dielectric soil moisture sensor. IEEE Trans. Geosci. Electron. GE-16(2) (1978) 112-118.

[61] TOMER, M.D., AND ANDERSON, J.L. Field evaluation of a soil water-capacitance probe in a fine sand. Soil Sci. 159(2) (1995) 90-98.

[62] MOHAMED, S.O., BERTUZZI, P., BRUAND, A., RAISON, L., AND BRUCKLER, L. Field evaluation and error analysis of soil water content measurement using the capacitance probe method. Soil Sci. Soc. Am. J. 61(2) (1997) 399-408.

[63] PALTINEANU, I.C., AND STARR, J.L. Real-time soil water dynamics using multisensor capacitance probes: Laboratory calibration. Soil Sci. Soc. Am. J. 61(6) (1997) 1576-1585.

[64] STARR, J.L., AND PALTINEANU, I.C. Soil water dynamics using multisensor capacitance probes in nontraffic interrows of corn. Soil Sci. Soc. Am. J. 62(1) (1998) 114-122.

Appendix A. BASIC code for setting TDR window width

```
SUB BestDistDv.Vp (ProbeLen, FtMtrs, Theta)
'Routine for choosing the best combination of Dist/Div and Vp for a given
'probe length based on inversion of Topp's equation for permittivity, Ka,
'as a function of water content.  Written in Microsoft BASIC 7.1 by S.R.
Evett
'ProbeLen is probe length in meters.
'FtMtrs 'If 1 then units are feet else units are m.
'Theta is volumetric water content (m^3/m^3).

SHARED Vp
SHARED Dist
SHARED DistDv
SHARED CardType%
i% = 10
DIM TimeErr(i%)
DIM DistVal(i%)

'Limit values of water content:
IF Theta < 0 THEN Theta = 0
IF Theta > .6 THEN Theta = .6
'Calculate the apparent permittivity (Ka) (Topp et al., 1980 [1]):
Ka = 3.03 + 9.3 * Theta + 146! * Theta * Theta - 76.7 * Theta *Theta *Theta
'The velocity of propagation is a function of Ka:
v = .299792 * 1E+09 / SQR(Ka)
'The travel time is a function of v and probe length:
tt = ProbeLen / v

'Assume that the travel time should occupy 70% of the screen max.
NewTtFull = (tt / .7) * 1E+09   'in ns

row% = CSRLIN
col% = POS(0)

TryAgain% = 0
SELECT CASE CardType%
CASE 5
Start.Search:
    'Try smallest Dist first, then next biggest, etc.
    'Get Dist for i=1 to 10:
    FOR i% = 0 TO 10
       DistDv = i%
       ReturnDistDv 'This returns one of the 11 possible Dist/Div settings.
       'Make sure DistM is in meters:  DistM is the distance per division.
       IF FtMtrs = 1 THEN
           'was in feet, convert to meters
           DistM = Dist * .3048
       ELSE
           'was in meters
           DistM = Dist
       END IF
       'Try biggest Vp first, then go to smallest
       FOR Vp = .99 TO .39 STEP -.01
           TtFull = DistM * 10 / (Vp * .2997925)
           IF TtFull >= NewTtFull THEN EXIT FOR
       NEXT Vp
       IF TtFull >= NewTtFull THEN EXIT FOR
    NEXT i%
    TimeError = (TtFull - NewTtFull) / NewTtFull
    BestDist = Dist
    IF ABS(TimeError) > .02 THEN
        PRINT "Best Dist/Div and Vp not found."
```

```
        PRINT "Error was"; TimeError * 100; "%"
        PressAKey (5)  'Wait for a key press before continuing.
    END IF
    'One combination of Vp and Dist/Div is known.
    'The Dist/Div value is in BestDist.  Print both Vp and Dist/Div:
    PRINT "        For VWC ="; Theta;
    LOCATE row% + 1, col%
    PRINT USING "recommend Vp: .## "; Vp;
    PRINT "and Dist/Div:"; BestDist;
    IF FtMtrs = 1 THEN
        PRINT "ft";
    ELSE
        PRINT "m";
    END IF

CASE ELSE
'For Tektronix 1502 cable tester, not 1502B/C.
'Provide two closest Dist/Div values for given Vp.
Start.Search2:
    'Get Dist for i=1 to 10:
    FOR i% = 0 TO 10
       DistDv = i%
       ReturnDistDv
       'Make sure DistM is in meters:
       IF FtMtrs = 1 THEN
           'feet
           DistM = Dist * .3048
       ELSE
           'meters
           DistM = Dist
       END IF
       'Use actual Vp first, and return error if TimeErr is too great
       TtFull = DistM * 10 / (Vp * .2997925)
       TimeErr(i% + 1) = (TtFull - NewTtFull) / NewTtFull
       DistVal(i% + 1) = Dist
       IF TimeErr(i% + 1) > 0 THEN EXIT FOR
    NEXT i%

    LOCATE 22, col%
    PRINT "For VWC ="; Theta;
    PRINT USING " and for Vp: .## "; Vp;
    FOR j% = i% TO i% + 1
        LOCATE 22 + 1 + j% - i%, col%
        PRINT "could use Dist/Div:"; DistVal(j%);
        IF FtMtrs = 1 THEN
            PRINT "ft";
        ELSE
            PRINT "m";
        END IF
        PRINT USING ". Error: ###"; TimeErr(j%) * 100;
        PRINT "%";
    NEXT j%
END SELECT
REDIM TimeErr(0)
REDIM DistVal(0)
END SUB
```

Appendix B. Finding travel times

Times t1.bis, t1, and t2 are reliably found by a combination of searches and decisions based on the results of those searches. In this discussion the wave form is assumed to consist of NP digitized data pairs of voltage and time with equal increments of time between consecutive data pairs.

1. Smooth data and first derivative using the Savitsky-Golay method and user set number of points, and find the maximum and minimum first derivative, maxDeriv and minDeriv.

2. Scan the wave form data from D2Lim to EndPt to find the lowest value, VMIN, and corresponding time, t2.1.

3. Scan the first derivative in a loop from StartPt to D1Lim to find the first maximum value, D1MAX, and associated time tD1MAX. If tD1MAX is greater than t2.1 then reduce D1Lim by NP/40 and try again. If D1Lim reaches 0 then write zeros to output.

4. Scan wave form data from tD1MAX+30 to EndPt for the lowest value, VMIN, and associated time, t2.1.

5. Scan wave form data from tD1MAX to tD1MAX + NP/8 to find the highest value, V1MAX, and associated time, t1p. Update V1MAX whenever the wave form value is higher than V1MAX and accumulate a count whenever the wave form value is lower. If count is greater than t1Swath then stop the search. This avoids finding the second peak if double peaks exist. If the wave form is continuously rising then t1p may be greater than tD1MAX + NP/20. If so then set t1p equal to tD1MAX + NP/20 and set V1MAX to the wave form value at that time.

6. Unless the global minimum method for finding t2 is forced, scan the derivative data from D2Lim to EndPt for the maximum derivative, D2MAX, and corresponding time, t2.2.

7. If the t2 derivative peak method is forced or if the t2 method is automatic and D2MAX is larger than D2Thresh then scan the data from t2.2 to t2.1 to find the zero derivative nearest to t2.2. Redefine t2.1 at this point and take the value of the wave form at this point as VMIN. If no zero derivative is found in this range of data then set t2.1 equal to t1p plus tatVMINFrac times the quantity (t2.2 - t1p) and set VMIN equal to the corresponding value of the wave form.

8. If the method for t2 is automatic and D2MAX is less than D2Thresh then set t2.2 equal to t2.1 plus the offset (RiseLimbOffset) specified by the user and set D2MAX equal to the corresponding value of the first derivative. Then set t2.1 equal to t1p plus tatVMINFrac times the quantity (t2.2 - t1p) and set VMIN equal to the corresponding value of the wave form.

9. If the local minimum method for t2 is forced then set t2.2 to t2.1 plus RiseLimbOffset (limited to less than or equal to NP) and set D2MAX to the corresponding value of the first derivative.

10. Regardless of how t2.2 is determined set Vt2.2 equal to the wave form value at t2.2.

11. Fit by linear regression a line to the base line between t2.1 and t2.1-BaseSwathWidth where BaseSwathWidth is a user chosen number of data points. If the slope of this line is positive then force a regression fit to the base line rather than a horizontal line tangent to VMIN.

12. Scan the derivative data from t1p to t1p plus t1Swath to find the lowest derivative value, DMIN, and corresponding time, tDMIN, which are associated with the descending limb of the first peak.

13. If DMIN is greater than -0.01 then set DMIN=(yll-yuu)/(xuu-xll), and set tDMIN equal to t1p + 1. The values of yll and yuu are the minimum and maximum of the wave form, respectively, and the values of xll and xuu are the minimum and maximum of the x-axis. Thus, the slope is scaled to the wave form amplitude.

14. Set VtDMIN equal to the wave form value at tDMIN, and if this value is greater than V1MAX then set VtDMIN to V1MAX.

15. Calculate the time of the intersection of tangent lines for t1 and if this time is less than t1p then increase the value of tDMIN and the magnitude of the slope, DMIN, until the intersection is at t1p or greater.

16. If t1 is less than the safety limit, SafetyLim, then write zeros to the file.

17. Set up limits on data used to fit tangent line to second rising limb as t2.2-Xinc and t2.2+Xinc where Xinc is user chosen. If these limits are out of range then write zeros to file.

19. If actual point to point slope near tD1MAX is greater than smoothed slope, D1MAX, then set D1MAX to actual maximum slope.

20. Examine derivative before first rising limb for slope close to zero (slope lesser in magnitude than [maxDeriv-minDeriv]/100). If such points are found then use the average wave form value for those points as the intercept for a line tangent to the baseline with slope of zero. If such points are not found then set the intercept of the horizontal line to the minimum wave form value to the left of tD1MAX.